



Diving below the Spin-down Limit: Constraints on Gravitational Waves from the Energetic Young Pulsar PSR J0537-6910

R. Abbott¹, T. D. Abbott², S. Abraham³, F. Acernese^{4,5}, K. Ackley⁶, A. Adams⁷, C. Adams⁸, R. X. Adhikari¹, V. B. Adya⁹, C. Affeldt^{10,11}, D. Agarwal³, M. Agathos^{12,13}, K. Agatsuma¹⁴, N. Aggarwal¹⁵, O. D. Aguiar¹⁶, L. Aiello^{17,18,19}, A. Ain^{20,21}, P. Ajith²², T. Akutsu^{23,24}, K. M. Aleman²⁵, G. Allen²⁶, A. Allocca^{5,27}, P. A. Altin⁹, A. Amato²⁸, S. Anand¹, A. Ananyeva¹, S. B. Anderson¹, W. G. Anderson²⁹, M. Ando^{23,30,31}, S. V. Angelova³², S. Ansoldi^{33,34}, J. M. Antelis³⁵, S. Antier³⁶, S. Appert¹, Koya Arai³⁷, Koji Arai¹, Y. Arai³⁷, S. Araki³⁸, A. Araya³⁹, M. C. Araya¹, J. S. Areeda²⁵, M. Arène³⁶, N. Aritomi³⁰, N. Arnaud^{40,41}, S. M. Aronson⁴², K. G. Arun⁴³, H. Asada⁴⁴, Y. Asali⁴⁵, G. Ashton⁶, Y. Aso^{46,47}, S. M. Aston⁸, P. Astone⁴⁸, F. Aubin⁴⁹, P. Aufmuth^{10,11}, K. AultO'Neal³⁵, C. Austin², S. Babak³⁶, F. Badaracco^{18,19}, M. K. M. Bader⁵⁰, S. Bae⁵¹, Y. Bae⁵², A. M. Baer⁷, S. Bagnasco⁵³, Y. Bai¹, L. Baiotti⁵⁴, J. Baird³⁶, R. Bajpai⁵⁵, M. Ball⁵⁶, G. Ballardini⁴¹, S. W. Ballmer⁵⁷, M. Bals³⁵, A. Balsamo⁷, G. Baltus⁵⁸, S. Banagiri⁵⁹, D. Bankar³, R. S. Bankar³, J. C. Barayoga¹, C. Barbieri^{60,61,62}, B. C. Barish¹, D. Barker⁶³, P. Barneo⁶⁴, S. Barnum⁶⁵, F. Barone^{5,66}, B. Barr⁶⁷, L. Barsotti⁶⁵, M. Barsuglia³⁶, D. Barta⁶⁸, J. Bartlett⁶³, M. A. Barton^{23,67}, I. Bartos⁴², R. Bassiri⁶⁹, A. Basti^{20,21}, M. Bawaj^{70,71}, J. C. Bayley⁶⁷, A. C. Baylor²⁹, M. Bazzan^{72,73}, B. Bécsy⁷⁴, V. M. Bedakihalé⁷⁵, M. Bejger⁷⁶, I. Belahcene⁴⁰, V. Benedetto⁷⁷, D. Beniwal⁷⁸, M. G. Benjamin³⁵, T. F. Bennett⁷⁹, J. D. Bentley¹⁴, M. BenYaala³², F. Bergamin^{10,11}, B. K. Berger⁶⁹, S. Bernuzzi¹³, D. Bersanetti⁸⁰, A. Bertolini⁸¹, J. Betzwieser⁸, R. Bhandare⁸¹, A. V. Bhandari³, D. Bhattacharjee⁸², S. Bhaumik⁴², J. Bidler²⁵, I. A. Bilenko⁸³, G. Billingsley¹, R. Birney⁸⁴, O. Birnholtz⁸⁵, S. Biscans^{1,65}, M. Bischl^{86,87}, S. Biscoveanu⁴, A. Bisht^{10,11}, B. Biswas³, M. Bitossi^{20,41}, M.-A. Bizouard⁸⁸, J. K. Blackburn¹, J. Blackman⁸⁹, C. D. Blair^{8,90}, D. G. Blair⁹⁰, R. M. Blair⁶³, F. Bobba^{91,92}, N. Bode^{10,11}, M. Boer⁸⁸, G. Bogaert⁸⁸, M. Boldrini^{48,93}, F. Bondu⁹⁴, E. Bonilla⁶⁹, R. Bonnand⁴⁹, P. Booker^{10,11}, B. A. Boom⁵⁰, R. Bork¹, V. Boschi²⁰, N. Bose⁹⁵, S. Bose³, V. Bossilkov⁹⁰, V. Boudart⁵⁸, Y. Bouffanais^{72,73}, A. Bozzi⁴¹, C. Bradaschia²⁰, P. R. Brady²⁹, A. Bramley⁸, A. Branch⁸, M. Branchesi^{18,19}, M. Breschi¹³, T. Briant⁹⁶, J. H. Briggs⁶⁷, A. Brillet⁸⁸, M. Brinkmann^{10,11}, P. Brockill²⁹, A. F. Brooks¹, J. Brooks⁴¹, D. D. Brown⁷⁸, S. Brunet¹, G. Bruno⁹⁷, R. H. Bruntz⁷, J. Bryant¹⁴, A. Buikema⁶⁵, T. Bulik⁹⁸, H. J. Bulten^{50,99}, A. Buonanno^{100,101}, R. Busicchio¹⁴, D. Buskulic⁴⁹, L. Cadonati¹⁰², M. Caesar¹⁰³, G. Cagnoli²⁸, C. Cahillane¹, H. W. Cain III², J. Calderón Bustillo¹⁰⁴, J. D. Callaghan⁶⁷, T. A. Callister^{105,106}, E. Calloni^{5,27}, J. B. Camp¹⁰⁷, M. Canepa^{80,108}, M. Cannavacciuolo⁹¹, K. C. Cannon³¹, H. Cao⁷⁸, J. Cao¹⁰⁹, Z. Cao¹¹⁰, E. Capocasa²³, E. Capote²⁵, G. Carapella^{91,92}, F. Carbognani⁴¹, J. B. Carlin¹¹¹, M. F. Carney¹⁵, M. Carpinelli^{112,113}, G. Carullo^{20,21}, T. L. Carver¹⁷, J. Casanueva Diaz⁴¹, C. Casentini^{114,115}, G. Castaldi¹¹⁶, S. Caudill^{50,117}, M. Cavaglia⁸², F. Cavalier⁴⁰, R. Cavalieri⁴¹, G. Cella²⁰, P. Cerdá-Durán¹¹⁸, E. Cesarini¹¹⁵, W. Chaibi⁸⁸, K. Chakravarti³, B. Champion¹¹⁹, C.-H. Chan¹²⁰, C. Chan³¹, C. L. Chan¹⁰⁴, M. Chan¹²¹, K. Chandra⁹⁵, P. Chanial⁴¹, S. Chao¹²⁰, P. Charlton¹²², E. A. Chase¹⁵, E. Chassande-Mottin³⁶, D. Chatterjee²⁹, M. Chaturvedi⁸¹, K. Chatziioannou^{1,105,106}, A. Chen¹⁰⁴, C. Chen^{123,124}, H. Y. Chen¹²⁵, J. Chen¹²⁰, K. Chen¹²⁶, X. Chen⁹⁰, Y.-B. Chen⁸⁹, Y.-R. Chen¹²⁴, Z. Chen¹⁷, H. Cheng⁴², C. K. Cheong¹⁰⁴, H. Y. Cheung¹⁰⁴, H. Y. Chia⁴², F. Chiadini^{92,127}, C.-Y. Chiang¹²⁸, R. Chierici¹²⁹, A. Chincarini⁸⁰, M. L. Chiofalo^{20,21}, A. Chiummo⁴¹, G. Cho¹³⁰, H. S. Cho¹³¹, S. Choate¹⁰³, R. K. Choudhary⁹⁰, S. Choudhary³, N. Christensen⁸⁸, H. Chu¹²⁶, Q. Chu⁹⁰, Y.-K. Chu¹²⁸, S. Chua⁹⁶, K. W. Chung¹³², G. Ciani^{72,73}, P. Cielciąg⁷⁶, M. Cieřlar⁷⁶, M. Cifaldi^{114,115}, A. A. Ciobanu⁷⁸, R. Ciolfi^{73,133}, F. Cipriano⁸⁸, A. Cirone^{80,108}, F. Clara⁶³, E. N. Clark¹³⁴, J. A. Clark¹⁰², L. Clarke¹³⁵, P. Clearwater¹¹¹, S. Clesse¹³⁶, F. Cleva⁸⁸, E. Coccia^{18,19}, P.-F. Cohadon⁹⁶, D. E. Cohen⁴⁰, L. Cohen², M. Colleoni¹³⁷, C. G. Collette¹³⁸, M. Colpi^{60,61}, C. M. Compton⁶³, M. Constancio Jr.¹⁶, L. Conti⁷³, S. J. Cooper¹⁴, P. Corban⁸, T. R. Corbitt², I. Cordero-Carrión¹³⁹, S. Corezzi^{70,71}, K. R. Corley⁴⁵, N. Cornish⁷⁴, D. Corre⁴⁰, A. Corsi¹⁴⁰, S. Cortese⁴¹, C. A. Costa¹⁶, R. Cotesta¹⁰¹, M. W. Coughlin⁵⁹, S. B. Coughlin^{15,17}, J.-P. Coulon⁸⁸, S. T. Countryman⁴⁵, B. Cousins¹⁴¹, P. Couvares¹, P. B. Covas¹³⁷, D. M. Coward⁹⁰, M. J. Cowart⁸, D. C. Coyne¹, R. Coyne¹⁴², J. D. E. Creighton²⁹, T. D. Creighton¹⁴³, A. W. Criswell⁵⁹, M. Croquette⁹⁶, S. G. Crowder¹⁴⁴, J. R. Cudell⁵⁸, T. J. Cullen², A. Cumming⁶⁷, R. Cummings⁶⁷, E. Cuoco^{20,41,145}, M. Curyło⁹⁸, T. Dal Canton^{40,101}, G. Dálya¹⁴⁶, A. Dana⁶⁹, L. M. DaneshgaranBajastani⁷⁹, B. D'Angelo^{80,108}, S. L. Danilishin¹⁴⁷, S. D'Antonio¹¹⁵, K. Danzmann^{10,11}, C. Darsow-Fromm¹⁴⁸, A. Dasgupta⁷⁵, L. E. H. Datrier⁶⁷, V. Dattilo⁴¹, I. Dave⁸¹, M. Davier⁴⁰, G. S. Davies^{149,150}, D. Davis¹, E. J. Daw¹⁵¹, R. Dean¹⁰³, M. Deenadayalan³, J. Degallaix¹⁵², M. De Laurentis^{5,27}, S. Deléglise⁹⁶, V. Del Favero¹¹⁹, F. De Lillo⁹⁷, N. De Lillo⁶⁷, W. Del Pozzo^{20,21}, L. M. DeMarchi¹⁵, F. De Matteis^{114,115}, V. D'Emilio¹⁷, N. Demos⁶⁵, T. Dent¹⁴⁹, A. Depasse⁹⁷, R. De Pietri^{153,154}, R. De Rosa^{5,27}, C. De Rossi⁴¹, R. DeSalvo¹¹⁶, R. De Simone¹²⁷, S. Dhurandhar³, M. C. Díaz¹⁴³, M. Diaz-Ortiz Jr.⁴², N. A. Didio⁵⁷, T. Dietrich¹⁰¹, L. Di Fiore⁵, C. Di Fronzo¹⁴, C. Di Giorgio^{91,92}, F. Di Giovanni¹¹⁸, T. Di Girolamo^{5,27}, A. Di Lieto^{20,21}, B. Ding¹³⁸, S. Di Pace^{48,93}, I. Di Palma^{48,93}, F. Di Renzo^{20,21}, A. K. Divakarla⁴², A. Dmitriev¹⁴, Z. Doctor⁵⁶, L. D'Onofrio^{5,27}, F. Donovan⁶⁵, K. L. Dooley¹⁷, S. Doravari³, I. Dorrington¹⁷, M. Drago^{18,19}, J. C. Driggers⁶³, Y. Drori¹, Z. Du¹⁰⁹, J.-G. Ducoin⁴⁰, P. Dupej⁶⁷, O. Durante^{91,92}, D. D'Urso^{112,113}, P.-A. Duverne⁴⁰, S. E. Dwyer⁶³, P. J. Easter⁶, M. Ebersold¹⁵⁵, G. Eddolls⁶⁷, B. Edelman⁵⁶, T. B. Edo^{1,151}, O. Edy¹⁵⁰, A. Effer⁸, S. Eguchi¹²¹, J. Eichholz⁹, S. S. Eikenberry⁴², M. Eisenmann⁴⁹, R. A. Eisenstein⁶⁵, A. Ejlli¹⁷, Y. Enomoto³⁰, L. Errico^{5,27}, R. C. Essick¹²⁵, H. Estellés¹³⁷, D. Estevez¹⁵⁶, Z. Etienne¹⁵⁷, T. Etzel¹, M. Evans⁶⁵, T. M. Evans⁸, B. E. Ewing¹⁴¹, V. Fafone^{18,114,115}, H. Fair⁵⁷, S. Fairhurst¹⁷, X. Fan¹⁰⁹, A. M. Farah¹²⁵, S. Farinon⁸⁰, B. Farr⁵⁶, W. M. Farr^{105,106}, N. W. Farrow⁶, E. J. Fauchon-Jones¹⁷, M. Favata¹⁵⁸, M. Fays^{58,151}, M. Fazio¹⁵⁹, J. Feicht¹, M. M. Fejer⁶⁹, F. Feng³⁶, E. Fenyvesi^{68,160}, D. L. Ferguson¹⁰², A. Fernandez-Galiana⁶⁵

I. Ferrante^{20,21}, T. A. Ferreira¹⁶, F. Fidecaro^{20,21}, P. Figura⁹⁸, I. Fiori⁴¹, M. Fishbach^{15,125}, R. P. Fisher⁷, J. M. Fishner⁶⁵, R. Fittipaldi^{92,161}, V. Fiumara^{92,162}, R. Flaminio^{23,49}, E. Floden⁵⁹, E. Flynn²⁵, H. Fong³¹, J. A. Font^{118,163}, B. Fornal¹⁶⁴, P. W. F. Forsyth⁹, A. Franke¹⁴⁸, S. Frasca^{48,93}, F. Frasconi²⁰, C. Frederick¹⁶⁵, Z. Frei¹⁴⁶, A. Freise¹⁶⁶, R. Frey⁵⁶, P. Fritschel⁶⁵, V. V. Frolov⁸, G. G. Fronzé⁵³, Y. Fujii¹⁶⁷, Y. Fujikawa¹⁶⁸, M. Fukunaga³⁷, M. Fukushima²⁴, P. Fulda⁴², M. Fyffe⁸, H. A. Gabbard⁶⁷, B. U. Gadre¹⁰¹, S. M. Gaebel¹⁴, J. R. Gair¹⁰¹, J. Gais¹⁰⁴, S. Galadage⁶, R. Gamba¹³, D. Ganapathy⁶⁵, A. Ganguly²², D. Gao¹⁶⁹, S. G. Gaonkar³, B. Garaventa^{80,108}, C. García-Núñez⁸⁴, C. García-Quirós¹³⁷, F. Garufi^{5,27}, B. Gateley⁶³, S. Gaudio³⁵, V. Gayathri⁴², G. Ge¹⁶⁹, G. Gemme⁸⁰, A. Gennai²⁰, J. George⁸¹, L. Gergely¹⁷⁰, P. Gewecke¹⁴⁸, S. Ghonge¹⁰², Abhirup Ghosh¹⁰¹, Archisman Ghosh¹⁷¹, Shaon Ghosh^{29,158}, Shrobana Ghosh¹⁷, Sourath Ghosh⁴², B. Giacomazzo^{60,61,62}, L. Giacoppo^{48,93}, J. A. Giaime^{2,8}, K. D. Giardino⁸, D. R. Gibson⁸⁴, C. Gier³², M. Giesler⁸⁹, P. Giri^{20,21}, F. Gissi⁷⁷, J. Glanzer², A. E. Gleckl²⁵, P. Godwin¹⁴¹, E. Goetz¹⁷², R. Goetz⁴², N. Gohlke^{10,11}, B. Goncharov⁶, G. González², A. Gopakumar¹⁷³, M. Gosselin⁴¹, R. Gouaty⁴⁹, B. Grace⁹, A. Grado^{5,174}, M. Granata¹⁵², V. Granata⁹¹, A. Grant⁶⁷, S. Gras⁶⁵, P. Grassia¹, C. Gray⁶³, R. Gray⁶⁷, G. Greco⁷⁰, A. C. Green⁴², R. Green¹⁷, A. M. Gretarsson³⁵, E. M. Gretarsson³⁵, D. Griffith¹, W. Griffiths¹⁷, H. L. Griggs¹⁰², G. Grignani^{70,71}, A. Grimaldi^{175,176}, E. Grimes³⁵, S. J. Grimm^{18,19}, H. Grote¹⁷, S. Grunewald¹⁰¹, P. Gruning⁴⁰, J. G. Guerrero²⁵, G. M. Guidi^{86,87}, A. R. Guimaraes², G. Guixé⁶⁴, H. K. Gulati⁷⁵, H.-K. Guo¹⁶⁴, Y. Guo⁵⁰, Anchal Gupta¹, Anuradha Gupta¹⁷⁷, P. Gupta^{50,117}, E. K. Gustafson¹, R. Gustafson¹⁷⁸, F. Guzman¹³⁴, S. Ha¹⁷⁹, L. Haegel³⁶, A. Hagiwara^{37,180}, S. Haino¹²⁸, O. Halim^{34,181}, E. D. Hall⁶⁵, E. Z. Hamilton¹⁷, G. Hammond⁶⁷, W.-B. Han¹⁸², M. Haney¹⁵⁵, J. Hanks⁶³, C. Hanna¹⁴¹, M. D. Hannam¹⁷, O. A. Hannuksela^{50,104,117}, H. Hansen⁶³, T. J. Hansen³⁵, J. Hanson⁸, T. Harder⁸⁸, T. Hardwick², K. Haris^{22,50,117}, J. Harms^{18,19}, G. M. Harry¹⁸³, I. W. Harry¹⁵⁰, D. Hartwig¹⁴⁸, K. Hasegawa³⁷, B. Haskell⁷⁶, R. K. Hasskew⁸, C.-J. Haster⁶⁵, K. Hattori¹⁸⁴, K. Haughian⁶⁷, H. Hayakawa¹⁸⁵, K. Hayama¹²¹, F. J. Hayes⁶⁷, J. Healy¹¹⁹, A. Heidmann⁹⁶, M. C. Heintze⁸, J. Heinze^{10,11}, J. Heinzl¹⁸⁶, H. Heitmann⁸⁸, F. Hellman¹⁸⁷, P. Hello⁴⁰, A. F. Helmling-Cornell⁵⁶, G. Hemming⁴¹, M. Hendry⁶⁷, I. S. Heng⁶⁷, E. Hennes⁵⁰, J. Hennig^{10,11}, M. H. Hennig^{10,11}, F. Hernandez Vivanco⁶, M. Heurs^{10,11}, S. Hild^{50,147}, P. Hill³², Y. Himemoto¹⁸⁸, A. S. Hines¹³⁴, Y. Hiranuma¹⁸⁹, N. Hirata²³, E. Hirose³⁷, W. C. G. Ho¹⁹⁰, S. Hochheim^{10,11}, D. Hofman¹⁵², J. N. Hohmann¹⁴⁸, A. M. Holgado²⁶, N. A. Holland⁹, I. J. Hollows¹⁵¹, Z. J. Holmes⁷⁸, K. Holt⁸, D. E. Holz¹²⁵, Z. Hong¹⁹¹, P. Hopkins¹⁷, J. Hough⁶⁷, E. J. Howell⁹⁰, C. G. Hoy¹⁷, D. Hoyland¹⁴, A. Hreibi^{10,11}, B. Hsieh³⁷, Y. Hsu¹²⁰, G.-Z. Huang¹⁹¹, H.-Y. Huang¹²⁸, P. Huang¹⁶⁹, Y.-C. Huang¹²⁴, Y.-J. Huang¹²⁸, Y.-W. Huang⁶⁵, M. T. Hübner⁶, A. D. Huddart¹³⁵, E. A. Huerta²⁶, B. Hughey³⁵, D. C. Y. Hui¹⁹², V. Hui⁴⁹, S. Husa¹³⁷, S. H. Huttner⁶⁷, R. Huxford¹⁴¹, T. Huynh-Dinh⁸, S. Ide¹⁹³, B. Idzkowski⁹⁸, A. Iess^{114,115}, B. Ikenoue²⁴, S. Imam¹⁹¹, K. Inayoshi¹⁹⁴, H. Inchauspe⁴², C. Ingram⁷⁸, Y. Inoue¹²⁶, G. Intini^{48,93}, K. Ioka¹⁹⁵, M. Isi⁶⁵, K. Isleif¹⁴⁸, K. Ito¹⁹⁶, Y. Itoh^{197,198}, B. R. Iyer²², K. Izumi¹⁹⁹, V. JaberianHamedan⁹⁰, T. Jacqmin⁹⁶, S. J. Jadhav²⁰⁰, S. P. Jadhav³, A. L. James¹⁷, A. Z. Jan¹¹⁹, K. Jani¹⁰², K. Janssens²⁰¹, N. N. Janthapur²⁰⁰, P. Jaranowski²⁰², D. Jariwala⁴², R. Jaume¹³⁷, A. C. Jenkins¹³², C. Jeon²⁰³, M. Jeunon⁵⁹, W. Jia⁶⁵, J. Jiang⁴², H.-B. Jin^{204,205}, G. R. Johns⁷, A. W. Jones⁹⁰, D. I. Jones²⁰⁶, J. D. Jones⁶³, P. Jones¹⁴, R. Jones⁶⁷, R. J. G. Jonker⁵⁰, L. Ju⁹⁰, K. Jung¹⁷⁹, P. Jung¹⁸⁵, J. Junker^{10,11}, K. Kaihotsu¹⁹⁶, T. Kajita²⁰⁷, M. Kakizaki¹⁸⁴, C. V. Kalaghatgi¹⁷, V. Kalogera¹⁵, B. Kamai¹, M. Kamiizumi¹⁸⁵, N. Kanda^{197,198}, S. Kandhasamy³, G. Kang⁵¹, J. B. Kanner¹, Y. Kao¹²⁰, S. J. Kapadia²², D. P. Kapasi⁹, C. Karathanasis²⁰⁸, S. Karki⁸², R. Kashyap¹⁴¹, M. Kasprzack¹, W. Kastaun^{10,11}, S. Katsanevas⁴¹, E. Katsavounidis⁶⁵, W. Katzman⁸, T. Kaur⁹⁰, K. Kawabe⁶³, K. Kawaguchi³⁷, N. Kawai²⁰⁹, T. Kawasaki³⁰, F. Kéfélian⁸⁸, D. Keitel¹³⁷, J. S. Key²¹⁰, S. Khadka⁶⁹, F. Y. Khalilil⁸³, I. Khan^{18,115}, S. Khan¹⁷, E. A. Khazanov²¹¹, N. Khetan^{18,19}, M. Khursheed⁸¹, N. Kijbunchoo⁹, C. Kim^{203,212}, J. C. Kim²¹³, J. Kim²¹⁴, K. Kim²¹⁵, W. S. Kim⁵², Y.-M. Kim¹⁷⁹, C. Kimball¹⁵, N. Kimura¹⁸⁰, P. J. King⁶³, M. Kinley-Hanlon⁶⁷, R. Kirchhoff^{10,11}, J. S. Kissel⁶³, N. Kita³⁰, H. Kitazawa¹⁹⁶, L. Kleybolte¹⁴⁸, S. Klimenko⁴², A. M. Kneen¹⁷², T. D. Knowles¹⁵⁷, E. Knyazev⁶⁵, P. Koch^{10,11}, G. Koekoek^{50,147}, Y. Kojima²¹⁶, K. Kokeyama¹⁸⁵, S. Koley⁵⁰, P. Kolitsidou¹⁷, M. Kolstein²⁰⁸, K. Komori^{30,65}, V. Kondrashov¹, A. K. H. Kong¹²⁴, A. Kontos²¹⁷, N. Koper^{10,11}, M. Korobko¹⁴⁸, K. Kotake¹²¹, M. Kovalam⁹⁰, D. B. Kozak¹, C. Kozakai⁴⁶, R. Kozu²¹⁸, V. Kringel^{10,11}, N. V. Krishnendu^{10,11}, A. Królak^{219,220}, G. Kuehn^{10,11}, F. Kuei¹²⁰, A. Kumar²⁰⁰, P. Kumar²²¹, Rahul Kumar⁶³, Rakesh Kumar⁷⁵, J. Kume³¹, K. Kuns⁶⁵, C. Kuo¹²⁶, H.-S. Kuo¹⁹¹, Y. Kuromiya¹⁹⁶, S. Kuroyanagi²²², K. Kusayanagi²⁰⁹, K. Kwak¹⁷⁹, S. Kwang²⁹, D. Laghi^{20,21}, E. Lalande²²³, T. L. Lam¹⁰⁴, A. Lamberts^{88,224}, M. Landry⁶³, B. B. Lane⁶⁵, R. N. Lang⁶⁵, J. Lange^{119,225}, B. Lantz⁶⁹, I. La Rosa⁴⁹, A. Lartaux-Vollard⁴⁰, P. D. Lasky⁶, M. Laxen⁸, A. Lazzarini¹, C. Lazzaro^{72,73}, P. Leaci^{48,93}, S. Leavey^{10,11}, Y. K. Leconte⁶³, H. K. Lee²²⁶, H. M. Lee²¹⁵, H. W. Lee²¹³, J. Lee¹³⁰, K. Lee⁶⁹, R. Lee¹²⁴, J. Lehmann^{10,11}, A. Lemaître²²⁷, E. Leon²⁵, M. Leonardi²³, N. Leroy⁴⁰, N. Letendre⁴⁹, Y. Levin⁶, J. N. Leviton¹⁷⁸, A. K. Y. Li¹, B. Li¹²⁰, J. Li¹⁵, K. L. Li¹²⁴, T. G. F. Li¹⁰⁴, X. Li⁸⁹, C.-Y. Lin²²⁸, F.-K. Lin¹²⁸, F.-L. Lin¹⁹¹, H. L. Lin¹²⁶, L. C.-C. Lin¹⁷⁹, F. Linde^{50,229}, S. D. Linker⁷⁹, J. N. Linley⁶⁷, T. B. Littenberg²³⁰, G. C. Liu¹²³, J. Liu^{10,11}, K. Liu¹²⁰, X. Liu²⁹, M. Llorens-Monteagudo¹¹⁸, R. K. L. Lo¹, A. Lockwood²³¹, M. L. Lollie², L. T. London⁶⁵, A. Longo^{232,233}, D. Lopez¹⁵⁵, M. Lorenzini^{114,115}, V. Lorette²³⁴, M. Lormand⁸, G. Losurdo²⁰, J. D. Lough^{10,11}, C. O. Lousto¹¹⁹, G. Lovelace²⁵, H. Lück^{10,11}, D. Lumaca^{114,115}, A. P. Lundgren¹⁵⁰, L.-W. Luo¹²⁸, R. Macas¹⁷, M. MacInnis⁶⁵, D. M. Macleod¹⁷, I. A. O. MacMillan¹, A. Macquet⁸⁸, I. Magaña Hernandez²⁹, F. Magaña-Sandoval⁴², C. Magazzù²⁰, R. M. Magee¹⁴¹, R. Maggiore¹⁴, E. Majorana^{48,93}, I. Maksimovic²³⁴, S. Maliakal¹, A. Malik⁸¹, N. Man⁸⁸, V. Mandic⁵⁹, V. Mangano^{48,93}, J. L. Mango²³⁵, G. L. Mansell^{63,65}, M. Manske²⁹, M. Mantovani⁴¹, M. Mapelli^{72,73}, F. Marchesoni^{70,236}, M. Marchio²³, F. Marion⁴⁹, Z. Mark⁸⁹, S. Márka⁴⁵, Z. Márka⁴⁵, C. Markakis¹², A. S. Markosyan⁶⁹, A. Markowitz¹, E. Maros¹, A. Marquina¹³⁹, S. Marsat³⁶, F. Martelli^{86,87}, I. W. Martin⁶⁷, R. M. Martin¹⁵⁸, M. Martinez²⁰⁸, V. Martinez²⁸, K. Martinovic¹³², D. V. Martynov¹⁴, E. J. Marx⁶⁵, H. Masalehdan¹⁴⁸, K. Mason⁶⁵, E. Massera¹⁵¹, A. Masserot⁴⁹, T. J. Massinger⁶⁵, M. Masso-Reid⁶⁷, S. Mastrogiovanni³⁶, A. Matas¹⁰¹, M. Mateu-Lucena¹³⁷, F. Matichard¹⁶⁵,

M. Matushechka^{10,11}, N. Mavalala⁶⁵, J. J. McCann⁹⁰, R. McCarthy⁶³, D. E. McClelland⁹, P. McClincy¹⁴¹, S. McCormick⁸, L. McCuller⁶⁵, G. I. McGhee⁶⁷, S. C. McGuire²³⁷, C. McIsaac¹⁵⁰, J. McIver¹⁷², D. J. McManus⁹, T. McRae⁹, S. T. McWilliams¹⁵⁷, D. Meacher²⁹, M. Mehmet^{10,11}, A. K. Mehta¹⁰¹, A. Melatos¹¹¹, D. A. Melchor²⁵, G. Mendell⁶³, A. Menendez-Vazquez²⁰⁸, C. S. Menoni¹⁵⁹, R. A. Mercer²⁹, L. Mereni¹⁵², K. Merfeld⁵⁶, E. L. Merilh⁶³, J. D. Merritt⁵⁶, M. Merzougui⁸⁸, S. Meshkov^{1,291}, C. Messenger⁶⁷, C. Messick²²⁵, P. M. Meyers¹¹¹, F. Meylahn^{10,11}, A. Mhaske³, A. Miani^{175,176}, H. Miao¹⁴, I. Michaloliakos⁴², C. Michel¹⁵², Y. Michimura³⁰, H. Middleton¹¹¹, L. Milano²⁷, A. L. Miller^{42,97}, M. Millhouse¹¹¹, J. C. Mills¹⁷, E. Milotti^{34,181}, M. C. Milovich-Goff⁷⁹, O. Minazzoli^{88,238}, Y. Minenkov¹¹⁵, N. Mio²³⁹, Ll. M. Mir²⁰⁸, A. Mishkin⁴², C. Mishra²⁴⁰, T. Mishra⁴², T. Mistry¹⁵¹, S. Mitra³, V. P. Mitrofanov⁸³, G. Mitselmakher⁴², R. Mittleman⁶⁵, O. Miyakawa¹⁸⁵, A. Miyamoto¹⁹⁷, Y. Miyazaki³⁰, K. Miyo¹⁸⁵, S. Miyoki¹⁸⁵, Geoffrey Mo⁶⁵, K. Mogushi⁸², S. R. P. Mohapatra⁶⁵, S. R. Mohite²⁹, I. Molina²⁵, M. Molina-Ruiz¹⁸⁷, M. Mondin⁷⁹, M. Montani^{86,87}, C. J. Moore¹⁴, D. Moraru⁶³, F. Morawski⁷⁶, A. More³, C. Moreno³⁵, G. Moreno⁶³, Y. Mori¹⁹⁶, S. Morisaki^{31,37}, Y. Moriwaki¹⁸⁴, B. Mours¹⁵⁶, C. M. Mow-Lowry¹⁴, S. Mozzon¹⁵⁰, F. Muciaccia^{48,93}, Arunava Mukherjee^{67,241}, D. Mukherjee¹⁴¹, Soma Mukherjee¹⁴³, Subroto Mukherjee⁷⁵, N. Mukund^{10,11}, A. Mullavey⁸, J. Munch⁷⁸, E. A. Muñiz⁵⁷, P. G. Murray⁶⁷, R. Musenich^{80,108}, S. L. Nadji^{10,11}, K. Nagano¹⁹⁹, S. Nagano²⁴², A. Nagar^{53,243}, K. Nakamura²³, H. Nakano²⁴⁴, M. Nakano³⁷, R. Nakashima²⁰⁹, Y. Nakayama¹⁸⁴, I. Nardecchia^{114,115}, T. Narikawa³⁷, L. Naticchioni⁴⁸, B. Nayak⁷⁹, R. K. Nayak²⁴⁵, R. Negishi¹⁸⁹, B. F. Neil⁹⁰, J. Neilson^{77,92}, G. Nelemans²⁴⁶, T. J. N. Nelson⁸, M. Nery^{10,11}, A. Neunzert²¹⁰, K. Y. Ng⁶⁵, S. W. S. Ng⁷⁸, C. Nguyen³⁶, P. Nguyen⁵⁶, T. Nguyen⁶⁵, L. Nguyen Quynh²⁴⁷, W.-T. Ni^{169,204,248}, S. A. Nichols², A. Nishizawa³¹, S. Nissanke^{50,249}, F. Nocera⁴¹, M. Noh¹⁷², M. Norman¹⁷, C. North¹⁷, S. Nozaki¹⁸⁴, L. K. Nuttall¹⁵⁰, J. Oberling⁶³, B. D. O'Brien⁴², Y. Obuchi²⁴, J. O'Dell¹³⁵, W. Ogaki³⁷, G. Oganesyan^{18,19}, J. J. Oh⁵², K. Oh¹⁹², S. H. Oh⁵², M. Ohashi¹⁸⁵, N. Ohishi⁴⁶, M. Ohkawa¹⁶⁸, F. Ohme^{10,11}, H. Ohta³¹, M. A. Okada¹⁶, Y. Okutani¹⁹³, K. Okutomi¹⁸⁵, C. Olivetto⁴¹, K. Oohara¹⁸⁹, C. Ooi³⁰, R. Oram⁸, B. O'Reilly⁸, R. G. Ormiston⁵⁹, N. D. Ormsby⁷, L. F. Ortega⁴², R. O'Shaughnessy¹¹⁹, E. O'Shea²²¹, S. Oshino¹⁸⁵, S. Ossokine¹⁰¹, C. Osthelder¹, S. Otabe²⁰⁹, D. J. Ottaway⁷⁸, H. Overmier⁸, A. E. Pace¹⁴¹, G. Pagano^{20,21}, M. A. Page⁹⁰, G. Pagliaroli^{18,19}, A. Pai⁹⁵, S. A. Pai⁸¹, J. R. Palamos⁵⁶, O. Palashov²¹¹, C. Palomba⁴⁸, K. Pan¹²⁴, P. K. Panda²⁰⁰, H. Pang¹²⁶, P. T. H. Pang^{50,117}, C. Pankow¹⁵, F. Pannarale^{48,93}, B. C. Pant⁸¹, F. Paoletti²⁰, A. Paoli⁴¹, A. Paolone^{48,250}, A. Parisi¹²³, J. Park²¹⁵, W. Parker^{8,237}, D. Pascucci⁵⁰, A. Pasqualetti⁴¹, R. Passaquieti^{20,21}, D. Passuello²⁰, M. Patel⁷, B. Patricelli^{20,41}, E. Payne⁶, T. C. Pechsiri⁴², M. Pedraza¹, M. Pegoraro⁷³, A. Pele⁸, F. E. Peña Arellano¹⁸⁵, S. Penn²⁵¹, A. Perego^{175,176}, A. Pereira²⁸, T. Pereira²⁵², C. J. Perez⁶³, C. Périgois⁴⁹, A. Perreca^{175,176}, S. Perriès¹²⁹, J. Petermann¹⁴⁸, D. Pettersen¹, H. P. Pfeiffer¹⁰¹, K. A. Pham⁵⁹, K. S. Phukon^{3,50,229}, O. J. Piccinni⁴⁸, M. Pichot⁸⁸, M. Piendibene^{20,21}, F. Piergiovanni^{86,87}, L. Pierini^{48,93}, V. Pierre^{77,92}, G. Pillant⁴¹, F. Pilo²⁰, L. Pinard¹⁵², I. M. Pinto^{77,92,253,254}, B. J. Piotrkowski²⁹, K. Piotrkowski⁹⁷, M. Pirello⁶³, M. Pitkin²⁵⁵, E. Placidi^{48,93}, W. Plastino^{232,233}, C. Pluchar¹³⁴, R. Poggiani^{20,21}, E. Polini⁴⁹, D. Y. T. Pong¹⁰⁴, S. Ponrathnam³, P. Popolizio⁴¹, E. K. Porter³⁶, J. Powell²⁵⁶, M. Pracchia⁴⁹, T. Pradier¹⁵⁶, A. K. Prajapati⁷⁵, K. Prasai⁶⁹, R. Prasanna²⁰⁰, G. Pratten¹⁴, T. Prestegard²⁹, M. Principe^{77,92,253}, G. A. Prodi^{176,257}, L. Prokhorov¹⁴, P. Proposito^{114,115}, L. Prudenzi¹⁰¹, A. Puecher^{50,117}, M. Punturo⁷⁰, F. Puosi^{20,21}, P. Puppo⁴⁸, M. Pürer¹⁰¹, H. Qi¹⁷, V. Quetschke¹⁴³, P. J. Quinonez³⁵, R. Quitzow-James⁸², F. J. Raab⁶³, G. Raaijmakers^{50,249}, H. Radkins⁶³, N. Radulesco⁸⁸, P. Raffai¹⁴⁶, S. X. Rail²²³, S. Raja⁸¹, C. Rajan⁸¹, K. E. Ramirez¹⁴³, T. D. Ramirez²⁵, A. Ramos-Buades¹⁰¹, J. Rana¹⁴¹, P. Rapagnani^{48,93}, U. D. Rapol²⁵⁸, B. Ratto³⁵, V. Raymond¹⁷, N. Raza¹⁷², M. Razzano^{20,21}, J. Read²⁵, L. A. Rees¹⁸³, T. Regimbau⁴⁹, L. Rei⁸⁰, S. Reid³², D. H. Reitze¹⁴², P. Relton¹⁷, P. Retegno^{53,259}, F. Ricci^{48,93}, C. J. Richardson³⁵, J. W. Richardson¹, L. Richardson¹³⁴, P. M. Ricker²⁶, G. Riemenschneider^{53,259}, K. Riles¹⁷⁸, M. Rizzo¹⁵, N. A. Robertson¹⁶⁷, R. Robie¹, F. Robinet⁴⁰, A. Rocchi¹¹⁵, J. A. Rocha²⁵, S. Rodriguez²⁵, R. D. Rodriguez-Soto³⁵, L. Rolland⁴⁹, J. G. Rollins¹, V. J. Roma⁵⁶, M. Romanelli⁹⁴, R. Romano^{4,5}, C. L. Romel⁶³, A. Romero²⁰⁸, I. M. Romero-Shaw⁶, J. H. Romie⁸, C. A. Rose²⁹, D. Rosińska⁹⁸, S. G. Rosofsky²⁶, M. P. Ross²³¹, S. Rowan⁶⁷, S. J. Rowlinson¹⁴, Santosh Roy³, Soumen Roy²⁶⁰, D. Rozza^{112,113}, P. Ruggi⁴¹, K. Ryan⁶³, S. Sachdev¹⁴¹, T. Sadecki⁶³, J. Sadiq¹⁴⁹, N. Sago²⁶¹, S. Saito²⁴, Y. Saito¹⁸⁵, K. Sakai²⁶², Y. Sakai¹⁸⁹, M. Sakellariadou¹³², Y. Sakuno¹²¹, O. S. Salafia^{60,61,62}, L. Salconi⁴¹, M. Saleem⁴³, F. Salemi^{175,176}, A. Samajdar^{50,117}, E. J. Sanchez¹, J. H. Sanchez²⁵, L. E. Sanchez¹, N. Sanchis-Gual²⁶³, J. R. Sanders²⁶⁴, A. Sanuy⁶⁴, T. R. Saravanan³, N. Sarin⁶, B. Sassolas¹⁵², H. Satari⁹⁰, S. Sato²⁶⁵, T. Sato¹⁶⁸, O. Sauter^{42,49}, R. L. Savage⁶³, V. Savant³, T. Sawada¹⁹⁷, D. Sawant⁹⁵, H. L. Sawant³, S. Sayah¹⁵², D. Schaetzl¹, M. Scheel⁸⁹, J. Scheuer¹⁵, A. Schindler-Tyka⁴², P. Schmidt¹⁴, R. Schnabel¹⁴⁸, M. Schneewind^{10,11}, R. M. S. Schofield⁵⁶, A. Schönbeck¹⁴⁸, B. W. Schulte^{10,11}, B. F. Schutz^{10,17}, E. Schwartz¹⁷, J. Scott⁶⁷, S. M. Scott⁹, M. Seglar-Arroyo⁴⁹, E. Seidel²⁶, T. Sekiguchi³¹, Y. Sekiguchi²⁶⁶, D. Sellers⁸, A. S. Sengupta²⁶⁰, N. Sennett¹⁰¹, D. Sentenac⁴¹, E. G. Seo¹⁰⁴, V. Sequino^{5,27}, Y. Setyawati^{10,11}, T. Shaffer⁶³, M. S. Shahriar¹⁵, B. Shams¹⁶⁴, L. Shao¹⁹⁴, S. Sharifi², A. Sharma^{18,19}, P. Sharma⁸¹, P. Shawhan¹⁰⁰, N. S. Shcheblanov²²⁷, H. Shen²⁶, S. Shibagaki¹²¹, M. Shikauchi³¹, R. Shimizu²⁴, T. Shimoda³⁰, K. Shimode¹⁸⁵, R. Shink²²³, H. Shinkai²⁶⁷, T. Shishido⁴⁷, A. Shoda²³, D. H. Shoemaker⁶⁵, D. M. Shoemaker²²⁵, K. Shukla¹⁸⁷, S. ShyamSundar⁸¹, M. Sieniawska⁹⁸, D. Sigg⁶³, L. P. Singer¹⁰⁷, D. Singh¹⁴¹, N. Singh⁹⁸, A. Singha^{50,147}, A. M. Sintes¹³⁷, V. Sipala^{112,113}, V. Skliris¹⁷, B. J. J. Slagmolen⁹, T. J. Slaven-Blair⁹⁰, J. Smetana¹⁴, J. R. Smith²⁵, R. J. E. Smith⁶, S. N. Somala²⁶⁸, K. Somiya²⁰⁹, E. J. Son⁵², K. Soni³, S. Soni², B. Sorazu⁶⁷, V. Sordini¹²⁹, F. Sorrentino⁸⁰, N. Sorrentino^{20,21}, H. Sotani²⁶⁹, R. Soulard⁸⁸, T. Souradeep^{3,258}, E. Sowell¹⁴⁰, V. Spagnuolo^{50,147}, A. P. Spencer⁶⁷, M. Spera^{72,73}, A. K. Srivastava⁷⁵, V. Srivastava⁵⁷, K. Staats¹⁵, C. Stachie⁸⁸, D. A. Steer³⁶, J. Steinlechner^{50,147}, S. Steinlechner^{50,147}, D. J. Stops¹⁴, M. Stover¹⁶⁵, K. A. Strain⁶⁷, L. C. Strang¹¹¹, G. Stratta^{87,270}, A. Strunk⁶³, R. Sturani²⁵², A. L. Stuver¹⁰³, J. Südbeck¹⁴⁸, S. Sudhagar³, V. Sudhir⁶⁵, R. Sugimoto^{199,271}, H. G. Suh²⁹, T. Z. Summerscales²⁷², H. Sun⁹⁰, L. Sun¹⁹, S. Sunil⁷⁵, A. Sur⁷⁶, J. Suresh^{31,37}, P. J. Sutton¹⁷, Takamasa Suzuki¹⁶⁸, Toshikazu Suzuki³⁷, B. L. Swinkels⁵⁰

M. J. Szczepańczyk⁴², P. Szewczyk⁹⁸, M. Tacca⁵⁰, H. Tagoshi³⁷, S. C. Tait⁶⁷, H. Takahashi²⁷³, R. Takahashi²³, A. Takamori³⁹, S. Takano³⁰, H. Takeda³⁰, M. Takeda¹⁹⁷, C. Talbot¹, H. Tanaka²⁷⁴, Kazuyuki Tanaka¹⁹⁷, Kenta Tanaka²⁷⁴, Taiki Tanaka³⁷, Takahiro Tanaka²⁶¹, A. J. Tanasijczuk⁹⁷, S. Tanioka^{23,47}, D. B. Tanner⁴², D. Tao¹, A. Tapia²⁵, E. N. Tapia San Martin²³, E. N. Tapia San Martin⁵⁰, J. D. Tasson¹⁸⁶, S. Telada²⁷⁵, R. Tenorio¹³⁷, L. Terkowski¹⁴⁸, M. Test²⁹, M. P. Thirugnanasambandam³, M. Thomas⁸, P. Thomas⁶³, J. E. Thompson¹⁷, S. R. Thondapu⁸¹, K. A. Thorne⁸, E. Thrane⁶, Shubhanshu Tiwari¹⁵⁵, Srishti Tiwari¹⁷³, V. Tiwari¹⁷, K. Toland⁶⁷, A. E. Tolley¹⁵⁰, T. Tomaru²³, Y. Tomigami¹⁹⁷, T. Tomura¹⁸⁵, M. Tonelli^{20,21}, A. Torres-Forné¹¹⁸, C. I. Torrie¹, I. Tosta e Melo^{112,113}, D. Töyrä⁹, A. Trapananti^{70,236}, F. Travasso^{70,236}, G. Traylor⁸, M. C. Tringali⁴¹, A. Tripathee¹⁷⁸, L. Troiano^{92,276}, A. Trovato³⁶, L. Trozzo¹⁸⁵, R. J. Trudeau¹, D. S. Tsai¹²⁰, D. Tsai¹²⁰, K. W. Tsang^{50,117,277}, T. Tsang¹⁰⁴, J.-S. Tsao¹⁹¹, M. Tse⁶⁵, R. Tso⁸⁹, K. Tsubono³⁰, S. Tsuchida¹⁹⁷, L. Tsukada³¹, D. Tsuna³¹, T. Tsutsui³¹, T. Tsuzuki²⁴, M. Turconi⁸⁸, D. Tuyenbayev¹²⁸, A. S. Ubhi¹⁴, N. Uchikata³⁷, T. Uchiyama¹⁸⁵, R. P. Udall^{1,102}, A. Ueda¹⁸⁰, T. Uehara^{278,279}, K. Ueno³¹, G. Ueshima²⁷³, D. Ugolini²⁸⁰, C. S. Unnikrishnan¹⁷³, F. Uraguchi²⁴, A. L. Urban², T. Ushiba³⁷, S. A. Usman¹²⁵, A. C. Utina^{50,147}, H. Vahlbruch^{10,11}, G. Vajente¹, A. Vajpeyi⁶, G. Valdes², M. Valentini^{175,176}, V. Valsan²⁹, N. van Bakel⁵⁰, M. van Beuzekom⁵⁰, J. F. J. van den Brand^{50,99,147}, C. Van Den Broeck^{50,117}, D. C. Vander-Hyde⁵⁷, L. van der Schaaf⁵⁰, J. V. van Heijningen^{90,97}, M. H. P. M. van Putten²⁸¹, M. Vardaro^{50,229}, A. F. Vargas¹¹¹, V. Varma⁸⁹, M. Vasúth⁶⁸, A. Vecchio¹⁴, G. Vedovato⁷³, J. Veitch⁶⁷, P. J. Veitch⁷⁸, K. Venkateswara²³¹, J. Venneberg^{10,11}, G. Venugopalan¹, D. Verkindt⁴⁹, Y. Verma⁸¹, D. Veske⁴⁵, F. Vetrano⁸⁶, A. Viceré^{86,87}, A. D. Viets²³⁵, V. Villa-Ortega¹⁴⁹, J.-Y. Vinet⁸⁸, S. Vitale⁶⁵, T. Vo⁵⁷, H. Vocca^{70,71}, E. R. G. von Reis⁶³, C. Vorvick⁶³, S. P. Vyatchanin⁸³, L. E. Wade¹⁶⁵, M. Wade¹⁶⁵, K. J. Wagner¹¹⁹, R. C. Walet⁵⁰, M. Walker⁷, G. S. Wallace³², L. Wallace¹, S. Walsh²⁹, J. Wang¹⁶⁹, J. Z. Wang¹⁷⁸, W. H. Wang¹⁴³, R. L. Ward⁹, J. Warner⁶³, M. Was⁴⁹, T. Washimi²³, N. Y. Washington¹, J. Watchi¹³⁸, B. Weaver⁶³, L. Wei^{10,11}, M. Weinert^{10,11}, A. J. Weinstein¹, R. Weiss⁶⁵, C. M. Weller²³¹, F. Wellmann^{10,11}, L. Wen⁹⁰, P. Weßels^{10,11}, J. W. Westhouse³⁵, K. Wette⁹, J. T. Whelan¹¹⁹, D. D. White²⁵, B. F. Whiting⁴², C. Whittle⁶⁵, D. Wilken^{10,11}, D. Williams⁶⁷, M. J. Williams⁶⁷, A. R. Williamson¹⁵⁰, J. L. Willis¹, B. Willke^{10,11}, D. J. Wilson¹³⁴, W. Winkler^{10,11}, C. C. Wipf¹, T. Wlodarczyk¹⁰¹, G. Woan⁶⁷, J. Woehler^{10,11}, J. K. Wofford¹¹⁹, I. C. F. Wong¹⁰⁴, J. Wrangel^{10,11}, C. Wu¹²⁴, D. S. Wu^{10,11}, H. Wu¹²⁴, S. Wu¹²⁴, D. M. Wysocki^{29,119}, L. Xiao¹, W.-R. Xu¹⁹¹, T. Yamada²⁷⁴, H. Yamamoto¹, Kazuhiro Yamamoto¹⁸⁴, Kohei Yamamoto²⁷⁴, T. Yamamoto¹⁸⁵, K. Yamashita¹⁸⁴, R. Yamazaki¹⁹³, F. W. Yang¹⁶⁴, L. Yang¹⁵⁹, Yang Yang⁴², Yi Yang²⁸², Z. Yang⁵⁹, M. J. Yap⁹, D. W. Yeeles¹⁷, A. B. Yelikar¹¹⁹, M. Ying¹²⁰, K. Yokogawa¹⁹⁶, J. Yokoyama^{30,31}, T. Yokozawa¹⁸⁵, A. Yoon⁷, T. Yoshioka¹⁹⁶, Hang Yu⁸⁹, Haocun Yu⁶⁵, H. Yuzurihara³⁷, A. Zadrożny²²⁰, M. Zanolin³⁵, S. Zeidler²⁸³, T. Zelenova⁴¹, J.-P. Zendri⁷³, M. Zevin¹⁵, M. Zhan¹⁶⁹, H. Zhang¹⁹¹, J. Zhang⁹⁰, L. Zhang¹, R. Zhang⁴², T. Zhang¹⁴, C. Zhao⁹⁰, G. Zhao¹³⁸, Yue Zhao¹⁶⁴, Yuhang Zhao²³, Z. Zhou¹⁵, X. J. Zhu⁶, Z.-H. Zhu¹¹⁰, M. E. Zucker^{1,65}, J. Zweizig¹

The LIGO Scientific Collaboration, the Virgo Collaboration and the KAGRA Collaboration,
D. Antonopoulos^{284,285}, Z. Arzoumanian²⁸⁶, T. Enoto²⁸⁷, C. M. Espinoza²⁸⁸, and S. Guillot^{289,290}

¹ LIGO, California Institute of Technology, Pasadena, CA 91125, USA

² Louisiana State University, Baton Rouge, LA 70803, USA

³ Inter-University Centre for Astronomy and Astrophysics, Pune 411007, India

⁴ Dipartimento di Farmacia, Università di Salerno, I-84084 Fisciano, Salerno, Italy

⁵ INFN, Sezione di Napoli, Complesso Universitario di Monte S. Angelo, I-80126 Napoli, Italy

⁶ OzGrav, School of Physics & Astronomy, Monash University, Clayton, VIC 3800, Australia

⁷ Christopher Newport University, Newport News, VA 23606, USA

⁸ LIGO Livingston Observatory, Livingston, LA 70754, USA

⁹ OzGrav, Australian National University, Canberra, ACT 0200, Australia

¹⁰ Max Planck Institute for Gravitational Physics (Albert Einstein Institute), D-30167 Hannover, Germany

¹¹ Leibniz Universität Hannover, D-30167 Hannover, Germany

¹² University of Cambridge, Cambridge CB2 1TN, UK

¹³ Theoretisch-Physikalisches Institut, Friedrich-Schiller-Universität Jena, D-07743 Jena, Germany

¹⁴ University of Birmingham, Birmingham B15 2TT, UK

¹⁵ Center for Interdisciplinary Exploration & Research in Astrophysics (CIERA), Northwestern University, Evanston, IL 60208, USA

¹⁶ Instituto Nacional de Pesquisas Espaciais, 12227-010 São José dos Campos, São Paulo, Brazil

¹⁷ Gravity Exploration Institute, Cardiff University, Cardiff CF24 3AA, UK

¹⁸ Gran Sasso Science Institute (GSSI), I-67100 L'Aquila, Italy

¹⁹ INFN, Laboratori Nazionali del Gran Sasso, I-67100 Assergi, Italy

²⁰ INFN, Sezione di Pisa, I-56127 Pisa, Italy

²¹ Università di Pisa, I-56127 Pisa, Italy

²² International Centre for Theoretical Sciences, Tata Institute of Fundamental Research, Bengaluru 560089, India

²³ Gravitational Wave Science Project, National Astronomical Observatory of Japan (NAOJ), Mitaka City, Tokyo 181-8588, Japan

²⁴ Advanced Technology Center, National Astronomical Observatory of Japan (NAOJ), Mitaka City, Tokyo 181-8588, Japan

²⁵ California State University Fullerton, Fullerton, CA 92831, USA

²⁶ NCSA, University of Illinois at Urbana-Champaign, Urbana, IL 61801, USA

²⁷ Università di Napoli "Federico II," Complesso Universitario di Monte S. Angelo, I-80126 Napoli, Italy

²⁸ Université de Lyon, Université Claude Bernard Lyon 1, CNRS, Institut Lumière Matière, F-69622 Villeurbanne, France

²⁹ University of Wisconsin-Milwaukee, Milwaukee, WI 53201, USA

³⁰ Department of Physics, The University of Tokyo, Bunkyo-ku, Tokyo 113-0033, Japan

³¹ Research Center for the Early Universe (RESCEU), The University of Tokyo, Bunkyo-ku, Tokyo 113-0033, Japan

³² SUPA, University of Strathclyde, Glasgow G1 1XQ, UK

³³ Dipartimento di Matematica e Informatica, Università di Udine, I-33100 Udine, Italy

³⁴ INFN, Sezione di Trieste, I-34127 Trieste, Italy

³⁵ Embry-Riddle Aeronautical University, Prescott, AZ 86301, USA

- ³⁶ Université de Paris, CNRS, Astroparticule et Cosmologie, F-75006 Paris, France
- ³⁷ Institute for Cosmic Ray Research (ICRR), KAGRA Observatory, The University of Tokyo, Kashiwa City, Chiba 277-8582, Japan
- ³⁸ Accelerator Laboratory, High Energy Accelerator Research Organization (KEK), Tsukuba City, Ibaraki 305-0801, Japan
- ³⁹ Earthquake Research Institute, The University of Tokyo, Bunkyo-ku, Tokyo 113-0032, Japan
- ⁴⁰ Université Paris-Saclay, CNRS/IN2P3, IJCLab, 91405 Orsay, France
- ⁴¹ European Gravitational Observatory (EGO), I-56021 Cascina, Pisa, Italy
- ⁴² University of Florida, Gainesville, FL 32611, USA
- ⁴³ Chennai Mathematical Institute, Chennai 603103, India
- ⁴⁴ Department of Mathematics and Physics, Hirosaki University, Hirosaki City, Aomori 036-8561, Japan
- ⁴⁵ Columbia University, New York, NY 10027, USA
- ⁴⁶ Kamioka Branch, National Astronomical Observatory of Japan (NAOJ), Kamioka-cho, Hida City, Gifu 506-1205, Japan
- ⁴⁷ The Graduate University for Advanced Studies (SOKENDAI), Mitaka City, Tokyo 181-8588, Japan
- ⁴⁸ INFN, Sezione di Roma, I-00185 Roma, Italy
- ⁴⁹ Univ. Grenoble Alpes, Laboratoire d'Annecy de Physique des Particules (LAPP), Université Savoie Mont Blanc, CNRS/IN2P3, F-74941 Annecy, France
- ⁵⁰ Nikhef, Science Park 105, 1098 XG Amsterdam, Netherlands
- ⁵¹ Korea Institute of Science and Technology Information (KISTI), Yuseong-gu, Daejeon 34141, Republic of Korea
- ⁵² National Institute for Mathematical Sciences, Daejeon 34047, Republic of Korea
- ⁵³ INFN Sezione di Torino, I-10125 Torino, Italy
- ⁵⁴ International College, Osaka University, Toyonaka City, Osaka 560-0043, Japan
- ⁵⁵ School of High Energy Accelerator Science, The Graduate University for Advanced Studies (SOKENDAI), Tsukuba City, Ibaraki 305-0801, Japan
- ⁵⁶ University of Oregon, Eugene, OR 97403, USA
- ⁵⁷ Syracuse University, Syracuse, NY 13244, USA
- ⁵⁸ Université de Liège, B-4000 Liège, Belgium
- ⁵⁹ University of Minnesota, Minneapolis, MN 55455, USA
- ⁶⁰ Università degli Studi di Milano-Bicocca, I-20126 Milano, Italy
- ⁶¹ INFN, Sezione di Milano-Bicocca, I-20126 Milano, Italy
- ⁶² INAF, Osservatorio Astronomico di Brera sede di Merate, I-23807 Merate, Lecco, Italy
- ⁶³ LIGO Hanford Observatory, Richland, WA 99352, USA
- ⁶⁴ Institut de Ciències del Cosmos, Universitat de Barcelona, C/ Martí i Franquès 1, E-08028 Barcelona, Spain
- ⁶⁵ LIGO, Massachusetts Institute of Technology, Cambridge, MA 02139, USA
- ⁶⁶ Dipartimento di Medicina, "Chirurgia e Odontoiatria Scuola Medica Salernitana," Università di Salerno, I-84081 Baronissi, Salerno, Italy
- ⁶⁷ SUPA, University of Glasgow, Glasgow G12 8QQ, UK
- ⁶⁸ Wigner RCP, RMKI, H-1121 Budapest, Konkoly Thege Miklós út 29-33, Hungary
- ⁶⁹ Stanford University, Stanford, CA 94305, USA
- ⁷⁰ INFN, Sezione di Perugia, I-06123 Perugia, Italy
- ⁷¹ Università di Perugia, I-06123 Perugia, Italy
- ⁷² Università di Padova, Dipartimento di Fisica e Astronomia, I-35131 Padova, Italy
- ⁷³ INFN, Sezione di Padova, I-35131 Padova, Italy
- ⁷⁴ Montana State University, Bozeman, MT 59717, USA
- ⁷⁵ Institute for Plasma Research, Bhat, Gandhinagar 382428, India
- ⁷⁶ Nicolaus Copernicus Astronomical Center, Polish Academy of Sciences, 00-716, Warsaw, Poland
- ⁷⁷ Dipartimento di Ingegneria, Università del Sannio, I-82100 Benevento, Italy
- ⁷⁸ OzGrav, University of Adelaide, Adelaide, SA 5005, Australia
- ⁷⁹ California State University, Los Angeles, 5151 State University Drive, Los Angeles, CA 90032, USA
- ⁸⁰ INFN, Sezione di Genova, I-16146 Genova, Italy
- ⁸¹ RRCAT, Indore, Madhya Pradesh 452013, India
- ⁸² Missouri University of Science and Technology, Rolla, MO 65409, USA
- ⁸³ Faculty of Physics, Lomonosov Moscow State University, Moscow 119991, Russia
- ⁸⁴ SUPA, University of the West of Scotland, Paisley PA1 2BE, UK
- ⁸⁵ Bar-Ilan University, Ramat Gan, 5290002, Israel
- ⁸⁶ Università degli Studi di Urbino "Carlo Bo," I-61029 Urbino, Italy
- ⁸⁷ INFN, Sezione di Firenze, I-50019 Sesto Fiorentino, Firenze, Italy
- ⁸⁸ Artemis, Université Côte d'Azur, Observatoire Côte d'Azur, CNRS, F-06304 Nice, France
- ⁸⁹ Caltech CaRT, Pasadena, CA 91125, USA
- ⁹⁰ OzGrav, University of Western Australia, Crawley, WA 6009, Australia
- ⁹¹ Dipartimento di Fisica "E.R. Caianiello," Università di Salerno, I-84084 Fisciano, Salerno, Italy
- ⁹² INFN, Sezione di Napoli, Gruppo Collegato di Salerno, Complesso Universitario di Monte S. Angelo, I-80126 Napoli, Italy
- ⁹³ Università di Roma "La Sapienza," I-00185 Roma, Italy
- ⁹⁴ Univ Rennes, CNRS, Institut FOTON - UMR6082, F-3500 Rennes, France
- ⁹⁵ Indian Institute of Technology Bombay, Powai, Mumbai 400 076, India
- ⁹⁶ Laboratoire Kastler Brossel, Sorbonne Université, CNRS, ENS-Université PSL, Collège de France, F-75005 Paris, France
- ⁹⁷ Université catholique de Louvain, B-1348 Louvain-la-Neuve, Belgium
- ⁹⁸ Astronomical Observatory Warsaw University, 00-478 Warsaw, Poland
- ⁹⁹ VU University Amsterdam, 1081 HV Amsterdam, Netherlands
- ¹⁰⁰ University of Maryland, College Park, MD 20742, USA
- ¹⁰¹ Max Planck Institute for Gravitational Physics (Albert Einstein Institute), D-14476 Potsdam, Germany
- ¹⁰² School of Physics, Georgia Institute of Technology, Atlanta, GA 30332, USA
- ¹⁰³ Villanova University, 800 Lancaster Avenue, Villanova, PA 19085, USA
- ¹⁰⁴ Faculty of Science, Department of Physics, The Chinese University of Hong Kong, Shatin, N.T., Hong Kong, People's Republic of China
- ¹⁰⁵ Stony Brook University, Stony Brook, NY 11794, USA
- ¹⁰⁶ Center for Computational Astrophysics, Flatiron Institute, New York, NY 10010, USA
- ¹⁰⁷ NASA Goddard Space Flight Center, Greenbelt, MD 20771, USA
- ¹⁰⁸ Dipartimento di Fisica, Università degli Studi di Genova, I-16146 Genova, Italy
- ¹⁰⁹ Tsinghua University, Beijing 100084, People's Republic of China
- ¹¹⁰ Department of Astronomy, Beijing Normal University, Beijing 100875, People's Republic of China
- ¹¹¹ OzGrav, University of Melbourne, Parkville, VIC 3010, Australia

- ¹¹² Università degli Studi di Sassari, I-07100 Sassari, Italy
¹¹³ INFN, Laboratori Nazionali del Sud, I-95125 Catania, Italy
¹¹⁴ Università di Roma Tor Vergata, I-00133 Roma, Italy
¹¹⁵ INFN, Sezione di Roma Tor Vergata, I-00133 Roma, Italy
¹¹⁶ University of Sannio at Benevento, I-82100 Benevento, Italy and INFN, Sezione di Napoli, I-80100 Napoli, Italy
¹¹⁷ Institute for Gravitational and Subatomic Physics (GRASP), Utrecht University, Princetonplein 1, 3584 CC Utrecht, Netherlands
¹¹⁸ Departamento de Astronomía y Astrofísica, Universitat de València, E-46100 Burjassot, València, Spain
¹¹⁹ Rochester Institute of Technology, Rochester, NY 14623, USA
¹²⁰ National Tsing Hua University, Hsinchu City 30013, Taiwan
¹²¹ Department of Applied Physics, Fukuoka University, Jonan, Fukuoka City, Fukuoka 814-0180, Japan
¹²² OzGrav, Charles Sturt University, Wagga Wagga, NSW 2678, Australia
¹²³ Department of Physics, Tamkang University, Danshui Dist., New Taipei City 25137, Taiwan
¹²⁴ Department of Physics and Institute of Astronomy, National Tsing Hua University, Hsinchu 30013, Taiwan
¹²⁵ University of Chicago, Chicago, IL 60637, USA
¹²⁶ Department of Physics, Center for High Energy and High Field Physics, National Central University, Zhongli District, Taoyuan City 32001, Taiwan
¹²⁷ Dipartimento di Ingegneria Industriale (DIIN), Università di Salerno, I-84084 Fisciano, Salerno, Italy
¹²⁸ Institute of Physics, Academia Sinica, Nankang, Taipei 11529, Taiwan
¹²⁹ Institut de Physique des 2 Infinis de Lyon (IP2I), CNRS/IN2P3, Université de Lyon, Université Claude Bernard Lyon 1, F-69622 Villeurbanne, France
¹³⁰ Seoul National University, Seoul 08826, Republic of Korea
¹³¹ Pusan National University, Busan 46241, Republic of Korea
¹³² King's College London, University of London, London WC2R 2LS, UK
¹³³ INAF, Osservatorio Astronomico di Padova, I-35122 Padova, Italy
¹³⁴ University of Arizona, Tucson, AZ 85721, USA
¹³⁵ Rutherford Appleton Laboratory, Didcot OX11 0DE, UK
¹³⁶ Université libre de Bruxelles, Avenue Franklin Roosevelt 50-1050 Bruxelles, Belgium
¹³⁷ Universitat de les Illes Balears, IAC3—IEEC, E-07122 Palma de Mallorca, Spain
¹³⁸ Université Libre de Bruxelles, Brussels 1050, Belgium
¹³⁹ Departamento de Matemáticas, Universitat de València, E-46100 Burjassot, València, Spain
¹⁴⁰ Texas Tech University, Lubbock, TX 79409, USA
¹⁴¹ The Pennsylvania State University, University Park, PA 16802, USA
¹⁴² University of Rhode Island, Kingston, RI 02881, USA
¹⁴³ The University of Texas Rio Grande Valley, Brownsville, TX 78520, USA
¹⁴⁴ Bellevue College, Bellevue, WA 98007, USA
¹⁴⁵ Scuola Normale Superiore, Piazza dei Cavalieri, 7-56126 Pisa, Italy
¹⁴⁶ MTA-ELTE Astrophysics Research Group, Institute of Physics, Eötvös University, Budapest 1117, Hungary
¹⁴⁷ Maastricht University, 6200 MD Maastricht, Netherlands
¹⁴⁸ Universität Hamburg, D-22761 Hamburg, Germany
¹⁴⁹ IGFAE, Campus Sur, Universidad de Santiago de Compostela, 15782 Spain
¹⁵⁰ University of Portsmouth, Portsmouth, PO1 3FX, UK
¹⁵¹ The University of Sheffield, Sheffield S10 2TN, UK
¹⁵² Laboratoire des Matériaux Avancés (LMA), Institut de Physique des 2 Infinis (IP2I) de Lyon, CNRS/IN2P3, Université de Lyon, Université Claude Bernard Lyon 1, F-69622 Villeurbanne, France
¹⁵³ Dipartimento di Scienze Matematiche, Fisiche e Informatiche, Università di Parma, I-43124 Parma, Italy
¹⁵⁴ INFN, Sezione di Milano Bicocca, Gruppo Collegato di Parma, I-43124 Parma, Italy
¹⁵⁵ Physik-Institut, University of Zurich, Winterthurerstrasse 190, 8057 Zurich, Switzerland
¹⁵⁶ Université de Strasbourg, CNRS, IPHC UMR 7178, F-67000 Strasbourg, France
¹⁵⁷ West Virginia University, Morgantown, WV 26506, USA
¹⁵⁸ Montclair State University, Montclair, NJ 07043, USA
¹⁵⁹ Colorado State University, Fort Collins, CO 80523, USA
¹⁶⁰ Institute for Nuclear Research, Hungarian Academy of Sciences, Bem tér 18/c, H-4026 Debrecen, Hungary
¹⁶¹ CNR-SPIN, c/o Università di Salerno, I-84084 Fisciano, Salerno, Italy
¹⁶² Scuola di Ingegneria, Università della Basilicata, I-85100 Potenza, Italy
¹⁶³ Observatori Astronòmic, Universitat de València, E-46980 Paterna, València, Spain
¹⁶⁴ The University of Utah, Salt Lake City, UT 84112, USA
¹⁶⁵ Kenyon College, Gambier, OH 43022, USA
¹⁶⁶ Vrije Universiteit Amsterdam, 1081 HV Amsterdam, Netherlands
¹⁶⁷ Department of Astronomy, The University of Tokyo, Mitaka City, Tokyo 181-8588, Japan
¹⁶⁸ Faculty of Engineering, Niigata University, Nishi-ku, Niigata City, Niigata 950-2181, Japan
¹⁶⁹ State Key Laboratory of Magnetic Resonance and Atomic and Molecular Physics, Innovation Academy for Precision Measurement Science and Technology (APM), Chinese Academy of Sciences, Xiao Hong Shan, Wuhan 430071, People's Republic of China
¹⁷⁰ University of Szeged, Dóm tér 9, Szeged 6720, Hungary
¹⁷¹ Universiteit Gent, B-9000 Gent, Belgium
¹⁷² University of British Columbia, Vancouver, BC V6T 1Z4, Canada
¹⁷³ Tata Institute of Fundamental Research, Mumbai 400005, India
¹⁷⁴ INAF, Osservatorio Astronomico di Capodimonte, I-80131 Napoli, Italy
¹⁷⁵ Università di Trento, Dipartimento di Fisica, I-38123 Povo, Trento, Italy
¹⁷⁶ INFN, Trento Institute for Fundamental Physics and Applications, I-38123 Povo, Trento, Italy
¹⁷⁷ The University of Mississippi, University, MS 38677, USA
¹⁷⁸ University of Michigan, Ann Arbor, MI 48109, USA
¹⁷⁹ Department of Physics, School of Natural Science, Ulsan National Institute of Science and Technology (UNIST), Ulsan-gun, Ulsan 44919, Republic of Korea
¹⁸⁰ Applied Research Laboratory, High Energy Accelerator Research Organization (KEK), Tsukuba City, Ibaraki 305-0801, Japan
¹⁸¹ Dipartimento di Fisica, Università di Trieste, I-34127 Trieste, Italy
¹⁸² Chinese Academy of Sciences, Shanghai Astronomical Observatory, Shanghai 200030, People's Republic of China
¹⁸³ American University, Washington, DC 20016, USA
¹⁸⁴ Faculty of Science, University of Toyama, Toyama City, Toyama 930-8555, Japan
¹⁸⁵ Institute for Cosmic Ray Research (ICRR), KAGRA Observatory, The University of Tokyo, Kamioka-cho, Gifu 506-1205, Japan

- ¹⁸⁶ Carleton College, Northfield, MN 55057, USA
- ¹⁸⁷ University of California, Berkeley, CA 94720, USA
- ¹⁸⁸ College of Industrial Technology, Nihon University, Narashino City, Chiba 275-8575, Japan
- ¹⁸⁹ Graduate School of Science and Technology, Niigata University, Nishi-ku, Niigata City, Niigata 950-2181, Japan
- ¹⁹⁰ Department of Physics and Astronomy, Haverford College, 370 Lancaster Ave, Haverford, PA 19041, USA
- ¹⁹¹ Department of Physics, National Taiwan Normal University, section 4, Taipei 116, Taiwan
- ¹⁹² Astronomy & Space Science, Chungnam National University, Yuseong-gu, Daejeon 34134, Republic of Korea
- ¹⁹³ Department of Physics and Mathematics, Aoyama Gakuin University, Sagami-hara City, Kanagawa 252-5258, Japan
- ¹⁹⁴ Kavli Institute for Astronomy and Astrophysics, Peking University, Haidian District, Beijing 100871, People's Republic of China
- ¹⁹⁵ Yukawa Institute for Theoretical Physics (YITP), Kyoto University, Sakyo-ku, Kyoto City, Kyoto 606-8502, Japan
- ¹⁹⁶ Graduate School of Science and Engineering, University of Toyama, Toyama City, Toyama 930-8555, Japan
- ¹⁹⁷ Department of Physics, Graduate School of Science, Osaka City University, Sumiyoshi-ku, Osaka City, Osaka 558-8585, Japan
- ¹⁹⁸ Nambu Yoichiro Institute of Theoretical and Experimental Physics (NITEP), Osaka City University, Sumiyoshi-ku, Osaka City, Osaka 558-8585, Japan
- ¹⁹⁹ Institute of Space and Astronautical Science (JAXA), Chuo-ku, Sagami-hara City, Kanagawa 252-0222, Japan
- ²⁰⁰ Directorate of Construction, Services & Estate Management, Mumbai 400094 India
- ²⁰¹ Universiteit Antwerpen, Prinsstraat 13, 2000 Antwerpen, Belgium
- ²⁰² University of Białystok, 15-424 Białystok, Poland
- ²⁰³ Department of Physics, Ewha Womans University, Seodaemun-gu, Seoul 03760, Republic of Korea
- ²⁰⁴ National Astronomical Observatories, Chinese Academic of Sciences, Chaoyang District, Beijing, People's Republic of China
- ²⁰⁵ School of Astronomy and Space Science, University of Chinese Academy of Sciences, Chaoyang District, Beijing, People's Republic of China
- ²⁰⁶ University of Southampton, Southampton SO17 1BJ, UK
- ²⁰⁷ Institute for Cosmic Ray Research (ICRR), The University of Tokyo, Kashiwa City, Chiba 277-8582, Japan
- ²⁰⁸ Institut de Física d'Altes Energies (IFAE), Barcelona Institute of Science and Technology, and ICREA, E-08193 Barcelona, Spain
- ²⁰⁹ Graduate School of Science and Technology, Tokyo Institute of Technology, Meguro-ku, Tokyo 152-8551, Japan
- ²¹⁰ University of Washington Bothell, Bothell, WA 98011, USA
- ²¹¹ Institute of Applied Physics, Nizhny Novgorod, 603950, Russia
- ²¹² Ewha Womans University, Seoul 03760, Republic of Korea
- ²¹³ Inje University Gimhae, South Gyeongsang 50834, Republic of Korea
- ²¹⁴ Department of Physics, Myongji University, Yongin 17058, Republic of Korea
- ²¹⁵ Korea Astronomy and Space Science Institute (KASI), Yuseong-gu, Daejeon 34055, Republic of Korea
- ²¹⁶ Department of Physical Science, Hiroshima University, Higashihiroshima City, Hiroshima 903-0213, Japan
- ²¹⁷ Bard College, 30 Campus Road, Annandale-On-Hudson, NY 12504, USA
- ²¹⁸ Institute for Cosmic Ray Research (ICRR), Research Center for Cosmic Neutrinos (RCCN), The University of Tokyo, Kamioka-cho, Hida City, Gifu 506-1205, Japan
- ²¹⁹ Institute of Mathematics, Polish Academy of Sciences, 00656 Warsaw, Poland
- ²²⁰ National Center for Nuclear Research, 05-400 Świerk-Otwock, Poland
- ²²¹ Cornell University, Ithaca, NY 14850, USA
- ²²² Institute for Advanced Research, Nagoya University, Furocho, Chikusa-ku, Nagoya City, Aichi 464-8602, Japan
- ²²³ Université de Montréal/Polytechnique, Montreal, QC H3T 1J4, Canada
- ²²⁴ Laboratoire Lagrange, Université Côte d'Azur, Observatoire Côte d'Azur, CNRS, F-06304 Nice, France
- ²²⁵ Department of Physics, University of Texas, Austin, TX 78712, USA
- ²²⁶ Department of Physics, Hanyang University, Seoul 04763, Republic of Korea
- ²²⁷ NAVIER, École des Ponts, Univ Gustave Eiffel, CNRS, Marne-la-Vallée, France
- ²²⁸ National Center for High-performance computing, National Applied Research Laboratories, Hsinchu Science Park, Hsinchu City 30076, Taiwan
- ²²⁹ Institute for High-Energy Physics, University of Amsterdam, Science Park 904, 1098 XH Amsterdam, Netherlands
- ²³⁰ NASA Marshall Space Flight Center, Huntsville, AL 35811, USA
- ²³¹ University of Washington, Seattle, WA 98195, USA
- ²³² Dipartimento di Matematica e Fisica, Università degli Studi Roma Tre, I-00146 Roma, Italy
- ²³³ INFN, Sezione di Roma Tre, I-00146 Roma, Italy
- ²³⁴ ESPCI, CNRS, F-75005 Paris, France
- ²³⁵ Concordia University Wisconsin, Mequon, WI 53097, USA
- ²³⁶ Università di Camerino, Dipartimento di Fisica, I-62032 Camerino, Italy
- ²³⁷ Southern University and A&M College, Baton Rouge, LA 70813, USA
- ²³⁸ Centre Scientifique de Monaco, 8 quai Antoine 1er, MC-98000, Monaco
- ²³⁹ Institute for Photon Science and Technology, The University of Tokyo, Bunkyo-ku, Tokyo 113-8656, Japan
- ²⁴⁰ Indian Institute of Technology Madras, Chennai 600036, India
- ²⁴¹ Saha Institute of Nuclear Physics, Bidhannagar, West Bengal 700064, India
- ²⁴² The Applied Electromagnetic Research Institute, National Institute of Information and Communications Technology (NICT), Koganei City, Tokyo 184-8795, Japan
- ²⁴³ Institut des Hautes Etudes Scientifiques, F-91440 Bures-sur-Yvette, France
- ²⁴⁴ Faculty of Law, Ryukoku University, Fushimi-ku, Kyoto City, Kyoto 612-8577, Japan
- ²⁴⁵ Indian Institute of Science Education and Research, Kolkata, Mohanpur, West Bengal 741252, India
- ²⁴⁶ Department of Astrophysics/IMAPP, Radboud University Nijmegen, P.O. Box 9010, 6500 GL Nijmegen, Netherlands
- ²⁴⁷ Department of Physics, University of Notre Dame, Notre Dame, IN 46556, USA
- ²⁴⁸ Department of Physics, National Tsing Hua University, Hsinchu 30013, Taiwan
- ²⁴⁹ GRAPPA, Anton Pannekoek Institute for Astronomy and Institute for High-Energy Physics, University of Amsterdam, Science Park 904, 1098 XH Amsterdam, Netherlands
- ²⁵⁰ Consiglio Nazionale delle Ricerche - Istituto dei Sistemi Complessi, Piazzale Aldo Moro 5, I-00185 Roma, Italy
- ²⁵¹ Hobart and William Smith Colleges, Geneva, NY 14456, USA
- ²⁵² International Institute of Physics, Universidade Federal do Rio Grande do Norte, Natal RN 59078-970, Brazil
- ²⁵³ Museo Storico della Fisica e Centro Studi e Ricerche "Enrico Fermi," I-00184 Roma, Italy
- ²⁵⁴ Department of Engineering, University of Sannio, Benevento 82100, Italy
- ²⁵⁵ Lancaster University, Lancaster LA1 4YW, UK
- ²⁵⁶ OzGrav, Swinburne University of Technology, Hawthorn, VIC 3122, Australia
- ²⁵⁷ Università di Trento, Dipartimento di Matematica, I-38123 Povo, Trento, Italy
- ²⁵⁸ Indian Institute of Science Education and Research, Pune, Maharashtra 411008, India

- ²⁵⁹ Dipartimento di Fisica, Università degli Studi di Torino, I-10125 Torino, Italy
²⁶⁰ Indian Institute of Technology, Palaj, Gandhinagar, Gujarat 382355, India
²⁶¹ Department of Physics, Kyoto University, Sakyou-ku, Kyoto City, Kyoto 606-8502, Japan
²⁶² Department of Electronic Control Engineering, National Institute of Technology, Nagaoka College, Nagaoka City, Niigata 940-8532, Japan
²⁶³ Centro de Astrofísica e Gravitação (CENTRA), Departamento de Física, Instituto Superior Técnico, Universidade de Lisboa, 1049-001 Lisboa, Portugal
²⁶⁴ Marquette University, 11420 W. Clybourn Street, Milwaukee, WI 53233, USA
²⁶⁵ Graduate School of Science and Engineering, Hosei University, Koganei City, Tokyo 184-8584, Japan
²⁶⁶ Faculty of Science, Toho University, Funabashi City, Chiba 274-8510, Japan
²⁶⁷ Faculty of Information Science and Technology, Osaka Institute of Technology, Hirakata City, Osaka 573-0196, Japan
²⁶⁸ Indian Institute of Technology Hyderabad, Sangareddy, Khandi, Telangana 502285, India
²⁶⁹ iTHEMS (Interdisciplinary Theoretical and Mathematical Sciences Program), The Institute of Physical and Chemical Research (RIKEN), Wako, Saitama 351-0198, Japan
²⁷⁰ INAF, Osservatorio di Astrofisica e Scienza dello Spazio, I-40129 Bologna, Italy
²⁷¹ Department of Space and Astronautical Science, The Graduate University for Advanced Studies (SOKENDAI), Sagami-hara, Kanagawa 252-5210, Japan
²⁷² Andrews University, Berrien Springs, MI 49104, USA
²⁷³ Department of Information and Management Systems Engineering, Nagaoka University of Technology, Nagaoka City, Niigata 940-2188, Japan
²⁷⁴ Institute for Cosmic Ray Research (ICRR), Research Center for Cosmic Neutrinos (RCCN), The University of Tokyo, Kashiwa City, Chiba 277-8582, Japan
²⁷⁵ National Metrology Institute of Japan, National Institute of Advanced Industrial Science and Technology, Tsukuba City, Ibaraki 305-8568, Japan
²⁷⁶ Dipartimento di Scienze Aziendali - Management and Innovation Systems (DISA-MIS), Università di Salerno, I-84084 Fisciano, Salerno, Italy
²⁷⁷ Van Swinderen Institute for Particle Physics and Gravity, University of Groningen, Nijenborgh 4, 9747 AG Groningen, Netherlands
²⁷⁸ Department of Communications Engineering, National Defense Academy of Japan, Yokosuka City, Kanagawa 239-8686, Japan
²⁷⁹ Department of Physics, University of Florida, Gainesville, FL 32611, USA
²⁸⁰ Trinity University, San Antonio, TX 78212, USA
²⁸¹ Department of Physics and Astronomy, Sejong University, Gwangjin-gu, Seoul 143-747, Republic of Korea
²⁸² Department of Electrophysics, National Chiao Tung University, Hsinchu, Taiwan
²⁸³ Department of Physics, Rikkyo University, Toshima-ku, Tokyo 171-8501, Japan
²⁸⁴ Nicolaus Copernicus Astronomical Center, Polish Academy of Sciences, ul. Bartycka 18, 00-716 Warsaw, Poland
²⁸⁵ Jodrell Bank Centre for Astrophysics, School of Physics and Astronomy, University of Manchester, Manchester M13 9PL, UK
²⁸⁶ X-Ray Astrophysics Laboratory, NASA Goddard Space Flight Center, Greenbelt, MD 20771, USA
²⁸⁷ Extreme Natural Phenomena RIKEN Hakubi Research Team, RIKEN Cluster for Pioneering Research, 2-1 Hirasawa, Wako, Saitama 351-0198, Japan
²⁸⁸ Departamento de Física, Universidad de Santiago de Chile, Avenida Ecuador 3493, 9170124 Estación Central, Santiago, Chile
²⁸⁹ IRAP, CNRS, 9 avenue du Colonel Roche, BP 44346, F-31028 Toulouse Cedex 4, France
²⁹⁰ Université de Toulouse, CNES, UPS-OMP, F-31028 Toulouse, France

Received 2020 December 24; revised 2021 April 27; accepted 2021 May 1; published 2021 May 31

Abstract

We present a search for quasi-monochromatic gravitational-wave signals from the young, energetic X-ray pulsar PSR J0537–6910 using data from the second and third observing runs of LIGO and Virgo. The search is enabled by a contemporaneous timing ephemeris obtained using Neutron star Interior Composition Explorer (NICER) data. The NICER ephemeris has also been extended through 2020 October and includes three new glitches. PSR J0537–6910 has the largest spin-down luminosity of any pulsar and exhibits frequent and strong glitches. Analyses of its long-term and interglitch braking indices provide intriguing evidence that its spin-down energy budget may include gravitational-wave emission from a time-varying mass quadrupole moment. Its 62 Hz rotation frequency also puts its possible gravitational-wave emission in the most sensitive band of the LIGO/Virgo detectors. Motivated by these considerations, we search for gravitational-wave emission at both once and twice the rotation frequency from PSR J0537–6910. We find no signal, however, and report upper limits. Assuming a rigidly rotating triaxial star, our constraints reach below the gravitational-wave spin-down limit for this star for the first time by more than a factor of 2 and limit gravitational waves from the $l = m = 2$ mode to account for less than 14% of the spin-down energy budget. The fiducial equatorial ellipticity is constrained to less than about 3×10^{-5} , which is the third best constraint for any young pulsar.

Key words: Gravitational waves

1. Introduction

The young (1–5 kyr) energetic pulsar PSR J0537–6910 (Wang & Gotthelf 1998; Chen et al. 2006) resides in the Large Magellanic Cloud at a distance of 49.6 kpc (Pietrzyński et al. 2019). Its pulsations are only detectable at X-ray energies, and the pulsar was first observed by Marshall et al. (1998) using the Rossi X-ray Timing Explorer (RXTE) during searches for pulsations from the remnant of SN1987A. Further observations with RXTE, prior to its decommissioning in early 2012, revealed that PSR J0537–6910 often undergoes sudden changes in rotation frequency, i.e., glitches, at a rate of more than three per year, and exhibits interesting interglitch behavior (Marshall et al. 2004;

Middleditch et al. 2006; Andersson et al. 2018; Antonopoulou et al. 2018; Ferdman et al. 2018). Observations of the pulsar resumed from 2017 to 2020 using the Neutron star Interior Composition Explorer (NICER) on board the International Space Station (Gendreau et al. 2012), which revealed more glitches and a continuation of the timing behavior seen with RXTE (Ho et al. 2020b).

PSR J0537–6910 is a particularly intriguing potential gravitational-wave source. It is the fastest-spinning known young pulsar (with rotation frequency $f_{\text{rot}} = 62\text{Hz}$), which places its gravitational-wave frequency f (e.g., at twice f_{rot} ; see Section 2.1) in the most sensitive band of ground-based gravitational-wave detectors. PSR J0537–6910 also has the highest spin-down luminosity ($\dot{E} = 4.9 \times 10^{38} \text{erg s}^{-1}$) among the ~ 2900 known pulsars in the ATNF Pulsar Catalogue (Manchester et al. 2005). Its spin-down

²⁹¹ Deceased, 2020 August.

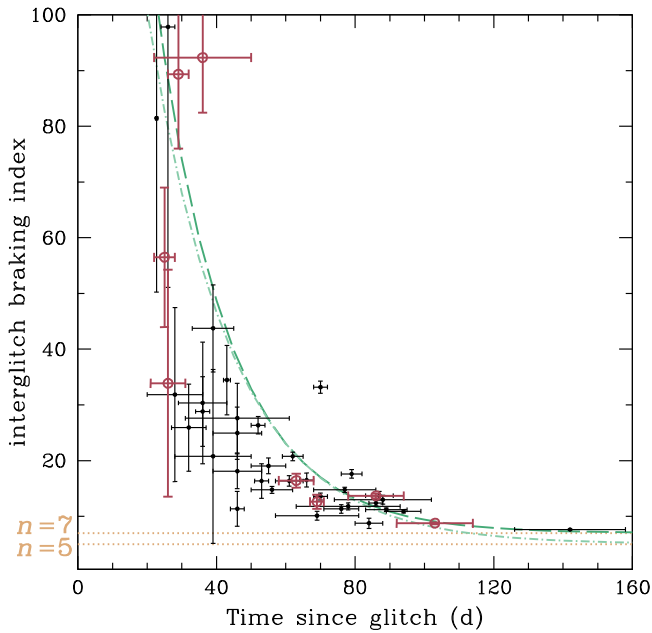


Figure 1. Interglitch braking index n_{ig} calculated from the spin parameters of each segment between glitches as a function of time since the last glitch. Large and small circles denote NICER and RXTE values, respectively, with the former from Tables 1 and 2 and from Ho et al. (2020b) and the latter from Antonopoulou et al. (2018). Errors in n_{ig} are 1σ uncertainty. Orange horizontal dotted lines indicate braking index $n = 5$ and 7 , which are expected for pulsar spin-down by gravitational-wave emission due to an ellipticity and r-mode oscillation, respectively. Green dotted-dashed and dashed lines indicate exponential decay to $n = 5$ with a best-fit timescale of 24 days and to $n = 7$ with a best-fit timescale of 21 days, respectively.

behavior appears to be driven by a process other than pure electromagnetic dipole radiation loss (at constant stellar magnetic field and moment of inertia). Specifically, its (long-term) braking index $n \equiv \dot{f}_{rot} \ddot{f}_{rot} / \dot{f}_{rot}^2 = -1.25 \pm 0.01$, as measured over more than 20 yr (Ho et al. 2020b), indicates an accelerating spin-down rate and significantly deviates from the measured values of most pulsars, $n = 3$, that imply dipole radiation (Shapiro & Teukolsky 1983).

More importantly, observations of PSR J0537–6910 show the pulsar’s (short-term) interglitch braking index n_{ig} , as measured during intervals between ~ 50 glitches, has values typically > 10 , and approaches an asymptotic value of $\lesssim 7$ at long times after a glitch, i.e., when the effects of a preceding glitch are diminished (see Figure 1; see also Andersson et al. 2018). It is this behavior that provides tantalizing suggestions that PSR J0537–6910 could be losing some of its rotational energy to gravitational-wave emission. In particular, a slightly deformed pulsar can emit gravitational waves that results in $n = 5$, and an r-mode fluid oscillation in a pulsar can emit gravitational waves that results in $n = 7$ (see, e.g., Riles 2017; Andersson et al. 2018; Glampedakis & Gualtieri 2018; Gao et al. 2020).

In this work, we search for mass quadrupolar gravitational-wave emission from PSR J0537–6910 that follows the same phase as that of the pulsar’s rotation. Previously, data from initial LIGO’s fifth and sixth science runs (S5 and S6) and Virgo’s second and fourth science runs (VSR2 and VSR4), in conjunction with RXTE timing measurements, were used to set limits on gravitational-wave emission by PSR J0537–6910 that closely approached the spin-down limit (Abbott et al. 2010; Aasi et al. 2014). Here, we analyze data from the second and

third observing runs (O2 and O3) of LIGO and Virgo, tracking the rotation phase with the contemporaneous NICER timing ephemeris. In doing so, we also provide an updated ephemeris that includes the latest six months of NICER observations of PSR J0537–6910.

Investigations of r-mode gravitational-wave emission ($n = 7$) are not presented here; such searches are more technically challenging and require different methods that search over a range of frequencies (see, e.g., Mytidis et al. 2015, 2019; Abbott et al. 2019b; Fesik & Papa 2020a, 2020b) due to uncertainty in gravitational-wave frequency for a given rotation frequency (Andersson et al. 2014; Idrisy et al. 2015; Caride et al. 2019). Nevertheless, we are able to reach below the spin-down limit of PSR J0537–6910 for the first time, which means that the minimum amplitude we could detect in our analysis is lower than the one obtained by assuming all of the pulsar’s rotational energy loss is converted to gravitational waves (see Section 2.1). In other words, we can now obtain physically meaningful constraints.

2. Search Method

2.1. Model of Gravitational-wave Emission

The first model considered here allows for gravitational-wave emission at once and twice the spin frequency simultaneously, which has been searched for previously (Pitkin et al. 2015; Abbott et al. 2017a, 2019a, 2020), and can result from a triaxial star spinning about an axis that is not its principal axis (Jones 2010, 2015). The amplitudes of each harmonic at once and twice the spin frequency of the star, denoted $h_{21}(t)$ and $h_{22}(t)$, respectively, can be written as

$$h_{21} = -\frac{C_{21}}{2} \{F_+^D(\alpha, \delta, \psi; t) \sin \iota \cos \iota \cos [\Phi(t) + \Phi_{21}^C] + F_\times^D(\alpha, \delta, \psi; t) \sin \iota \sin [\Phi(t) + \Phi_{21}^C]\}, \quad (1)$$

$$h_{22} = -C_{22} \{F_+^D(\alpha, \delta, \psi; t) (1 + \cos^2 \iota) \cos [2\Phi(t) + \Phi_{22}^C] + 2F_\times^D(\alpha, \delta, \psi; t) \cos \iota \sin [2\Phi(t) + \Phi_{22}^C]\}. \quad (2)$$

Here, C_{21} and C_{22} are dimensionless constant component amplitudes, and Φ_{21}^C and Φ_{22}^C are phase angles. F_+^D and F_\times^D are antenna or beam functions and describe how the two polarization components of the signal are projected onto the detector (see, e.g., Jaranowski et al. 1998). The angles (α, δ) are the R.A. and decl. of the source, while the angles (ι, ψ) specify the orientation of the star’s spin axis relative to the observer. $\Phi(t)$ is the rotational phase of the source.

The second model is a special case of the first model and is used for gravitational-wave emission at only twice the rotational frequency ($C_{21} = 0$), implying a triaxial star that is spinning about a principal axis, such as its z -axis. In this case, it is simpler to write the gravitational-wave amplitude in terms of the dimensionless value h_0 , which requires substituting $C_{22} = -h_0/2$ in Equation (2) (Abbott et al. 2019a). The sign change simply maintains consistency with the model from Jaranowski et al. (1998). The cause of such gravitational-wave emission is a deviation from axial symmetry, which can be written in terms of a dimensionless equatorial ellipticity ε , defined in terms of the star’s principal moments of inertia

Table 1
Timing Model Parameters for Segments between Epochs of New Glitches of PSR J0537–6910

Segment	Epoch (MJD)	Start (MJD)	End (MJD)	TOAs	f_{rot} (Hz)	\dot{f}_{rot} (10^{-10} Hz s $^{-1}$)	\ddot{f}_{rot} (10^{-20} Hz s $^{-2}$)	n_{ig}	Residual rms (μ s)	χ^2/dof
8	58931	58871.5	58991.2	17	61.908808739(3)	−1.997535(7)	1.06(8)	16(1)	173.7	9.9
9	59020	58995.6	59046.3	11	61.907273376(2)	−1.99699(4)	[1] ^a	...	147.8	6.7
10	59074	59050.4	59098.7	10	61.906349948(5)	−1.99762(2)	3.6(8)	56(13)	60.9	1.5
11	59129	59108.7	59150.7	11	61.905434556(6)	−1.99809(3)	2.2(13)	34(20)	72.3	2.1

Note. Columns from left to right are segment number, timing model epoch, segment start and end dates, number of times of arrival, rotation frequency and its first two time derivatives, interglitch braking index, and timing model residual and goodness-of-fit measure. Number in parentheses is 1σ uncertainty in last digit. Segments 1–7 are presented in Ho et al. (2020b).

^a \dot{f}_{rot} is fixed at 10^{-20} Hz s $^{-2}$.

(I_{xx}, I_{yy}, I_{zz}) :

$$\varepsilon \equiv \frac{|I_{xx} - I_{yy}|}{I_{zz}}. \quad (3)$$

The gravitational-wave amplitude is directly proportional to the ellipticity:

$$h_0 = \frac{16\pi^2 G}{c^4} \frac{I_{zz} \varepsilon f_{\text{rot}}^2}{d}, \quad (4)$$

where d is the star’s distance from the Earth. When setting upper limits, we use a fiducial value for the z-component of the moment of inertia, i.e., $I_{zz}^{\text{fid}} = 10^{38}$ kg m 2 . The combination of the ellipticity and fiducial moment of inertia can be cast in terms of the mass quadrupole moment of the $l = m = 2$ mode of the star via $Q_{22} = \sqrt{15/8\pi} I_{zz} \varepsilon$ (Owen 2005). The gravitational-wave amplitude h_0 can be compared to the spin-down limit amplitude h_0^{sd} , which is the gravitational-wave amplitude produced assuming that all of the rotational energy lost by the pulsar is converted into gravitational waves:

$$h_0^{\text{sd}} = \frac{1}{d} \left(\frac{5GI_{zz}}{2c^3} \frac{|\dot{f}_{\text{rot}}|}{f_{\text{rot}}} \right)^{1/2}. \quad (5)$$

Our results for the single harmonic case are quoted in terms of h_0^{sd} .

NICER observations of PSR J0537–6910 allow for the ephemeris of the pulsar to be determined, which means we know the expected signal frequency and its evolution. With this information, we can perform a targeted search for gravitational waves from this pulsar based on the two signal models discussed, with the phase tracking that of the pulsar rotation.

2.2. NICER Data

In Ho et al. (2020b), timing analysis is performed on NICER data of PSR J0537–6910 from 2017 August 17 to 2020 April 25, with eight glitches detected during this timespan and the last three glitches during O3. Here we present an update and results on timing analysis since the work of Ho et al. (2020b). In particular, data from 2020 May 12 to October 29 are analyzed using the methodology as described in Ho et al. (2020b). Our analysis reveals continuing accelerated spin-down (see Table 1) and three subsequent glitches (see Table 2 and Figure 2), including the smallest glitch of PSR J0537–6910 yet detected using NICER. Note that the timing model of segment 8 uses three additional subsequent times of arrival (TOAs)

Table 2
Parameters of New Glitches of PSR J0537–6910

Glitch	Glitch Epoch (MJD)	$\Delta\phi$ (cycle)	Δf_{rot} (μ Hz)	$\Delta \dot{f}_{\text{rot}}$ (10^{-13} Hz s $^{-1}$)	$\Delta \ddot{f}_{\text{rot}}$ (10^{-20} Hz s $^{-2}$)
8	58868(5)	0.08(12)	24.0(1)	−2.3(6)	−5(1)
9	58993(3)	0.06(12)	0.4(1)	−0.3(8)	...
10	59049(3)	−0.22(2)	8.46(3)	−1.3(5)	...
11	59103(5)	0.42(2)	33.958(7)	−2.0(3)	...

Note. Columns from left to right are glitch number and epoch, change in rotation phase and changes in rotation frequency, and its first two time derivatives at each glitch. Number in parentheses is 1σ uncertainty in last digit. Glitches 1–7 are presented in Ho et al. (2020b).

beyond those in Table 1 of Ho et al. (2020b) and, as a result, the epoch and other parameters of the model differ; e.g., segment 8 is associated with the data point at 63 days and $n_{\text{ig}} = 16$ in Figure 1 compared to 50 days and $n_{\text{ig}} = 22$ in Figure 6 of Ho et al. (2020b). Meanwhile, the relatively short timespan of segment 9 means the timing model for this segment is not able to constrain \dot{f}_{rot} . For the most recent glitch 11, its magnitude is large ($\Delta f_{\text{rot}} = 33.9\mu$ Hz), which suggests the time to the next glitch will be long ($\sim 200 \pm 20$ days; Ho et al. 2020b). If the interglitch period is indeed long, then NICER measurements could eventually yield $n_{\text{ig}} \lesssim 7$ for segment 11, which would lend further support for gravitational-wave emission (see Section 1 and Figure 1).

The gravitational-wave search performed here uses the timing model of Ho et al. (2020b). The differences between the model of Ho et al. (2020b) and the model presented here are well within the former’s uncertainties, and thus use of the latter would not yield significantly different results.

2.3. LIGO and Virgo Data

We use a combination of data from the second and third observing runs of the Advanced LIGO (Aasi et al. 2015) and Virgo (Acernese et al. 2015) gravitational-wave detectors. During O2, LIGO Livingston (L1) and LIGO Hanford (H1) took data from 2016 November 30 to 2017 August 25 and had duty factors of $\sim 57\%$ and $\sim 59\%$, respectively (including commissioning breaks), while Virgo took data from 2017 August 1 to 2017 August 25 with a duty factor of $\sim 85\%$. As noted in Section 2.2, NICER data start on 2017 August 17, and thus one set of searches we undertake uses only about six days of O2 data overlapping with the NICER data in addition to the O3 data (explicitly 5.3, 5.5, and 6.0 days of data for H1, L1,

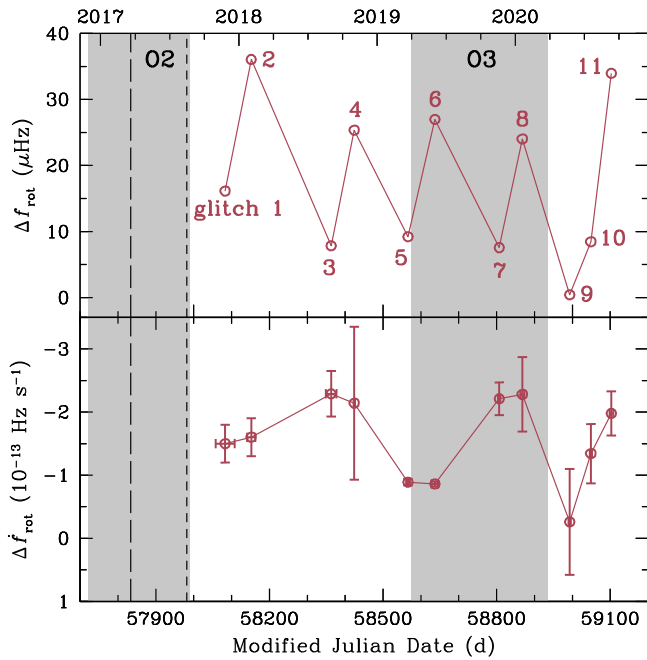


Figure 2. Glitch Δf_{rot} (top) and $\dot{\Delta f}_{\text{rot}}$ (bottom) as functions of time. Glitch numbers and values from Table 2 and Ho et al. (2020b). Errors in $\dot{\Delta f}_{\text{rot}}$ are 1σ uncertainty, while errors in Δf_{rot} are not shown because they are generally smaller than the symbols. Shaded regions denote second observing run (O2) and third observing run (O3) of LIGO/Virgo. Vertical long- and short-dashed lines indicate two possible start dates of O2 data used in the present work (see Section 2.3).

and V1, respectively). Alternatively, we can consider a more optimistic and much longer time series of O2 data by taking advantage of the correlation between glitch size and time to next glitch seen for PSR J0537–6910 (Middleditch et al. 2006; Antonopoulou et al. 2018; Ferdman et al. 2018; Ho et al. 2020b). Assuming a (unobserved) glitch occurred on 2017 March 22 with the same size as the largest NICER glitch (i.e., glitch 2 with $\Delta f_{\text{rot}} = 36\mu\text{Hz}$), we would expect a subsequent glitch 224 days later (at 68% confidence) on 2017 November 1, which is the earliest estimated date at which glitch 1 occurred (see Figure 2 and Ho et al. 2020b). Thus, 2017 March 22 to November 1 is the longest period over which we would expect PSR J0537–6910 to not have undergone a glitch and the NICER ephemeris to be valid. O3 lasted from 2019 April 1 to 2020 March 27, with a one-month pause in data collection in 2019 October. The three detectors’ data sets H1, L1, and V1 had duty factors of $\sim 72\%$, $\sim 69\%$, and $\sim 69\%$, or 259, 248, and 248 days of data, respectively, during O3.

In the case of a detection, calibration uncertainties limit our ability to provide robust estimates of the amplitude of the gravitational-wave signal and corresponding ellipticity (Abbott et al. 2017b). Even without a detection, these uncertainties affect the estimated instrument sensitivity and inferred upper limits. The uncertainties vary over the course of a run but do not change by large values, so we do not explicitly consider time-dependent calibration uncertainties in our analysis. For further information on O2 calibration techniques, see discussions in Abbott et al. (2019a).

The full raw strain data from the O2 run are publicly available from the Gravitational Wave Open Science Center²⁹²

(Vallisneri et al. 2015; Abbott et al. 2021). For the LIGO O3 data set, the analysis uses the “C01” calibration. The C01 calibration has estimated maximum amplitude and phase uncertainties of $\sim 7\%$ and $\sim 4^\circ$, respectively (Sun et al. 2020), which we use as conservative estimates of the true calibration uncertainty near the frequencies analyzed here. For the Virgo O3 data set, we use the “V0” calibration with estimated maximum amplitude and phase uncertainties of 5% and 2° , respectively.

2.4. Search Pipeline

The time-domain Bayesian method performs a coherent analysis of the interferometers’ data, meaning that we analyze the entire data set with an effective single Fourier Transform, thereby preserving the phase information. First, the raw strain data are heterodyned (Dupuis & Woan 2005) using the expected signal phase evolution, known precisely from the electromagnetic timing ephemeris. Then a low-pass filter with a knee frequency of 0.25 Hz is applied, and the data are downsampled so that the sampling time is 1 minute, compared to 60 ms originally. This heterodyning is performed for an expected signal whose frequency is at once or twice the rotational frequency of the pulsar. The heterodyned data are the input to a nested sampling algorithm that is a part of the LALINFERENCE package (Veitch & Vecchio 2010; Veitch et al. 2015), which infers the unknown signal parameters depending on the model of gravitational-wave emission.

PSR J0537–6910 glitched three times over the course of the gravitational-wave observations (see Figure 2). For each glitch, we assume an unknown phase offset between the electromagnetic and gravitational-wave phase. The individual phase offsets of multiple glitches that occurred between O2 and O3 cannot be disentangled, so only one phase offset is included for these glitches. This means that we introduce four additional phase parameters when performing parameter estimation.

We also make use of restricted and unrestricted priors when performing the analysis. In the first case, we use estimates of the orientation of the pulsar relative to the Earth based on a model fit of the observed pulsar wind nebulae torus (Ng & Romani 2008), which imply narrow priors in our analysis on the polarization and inclination angles. Therefore, we use a Gaussian prior on ψ of 2.2864 ± 0.0384 rad and a bimodal Gaussian prior on ι with modes at 1.522 ± 0.016 and 1.620 ± 0.016 rad (see Jones 2015, for reasons behind the bimodality). This range of ι would suggest the pulsar’s rotation axis is almost perpendicular to the line of sight, which would in turn lead to a linearly polarized gravitational-wave signal dominated by the “+” polarization component. The second case assumes a uniform isotropic prior on the axis direction, which therefore does not rely on assumptions about the pulsar’s orientation matching that of the wind nebula or uncertainties in the above modeling of the not-well-resolved X-ray observations. The initial signal phase and glitch phase offsets all use uniform priors over their full ranges. For the single harmonic search, we parameterize the signals using the mass quadrupole Q_{22} and distance. As a conservative approach, we use an unphysical flat prior on Q_{22} with a lower bound at zero and an upper bound of 5×10^{37} kg m², which is well above the largest upper limits found in Abbott et al. (2019a). For the distance, we use a Gaussian prior with mean of 49.59 kpc and standard deviation of 0.55 kpc based on the value given in Pietrzyński et al. (2019), combining the statistical and systematic errors in quadrature. For the dual harmonic search, which uses the amplitudes C_{21} and C_{22} rather than the physical parameters of

²⁹² <https://www.gw-open-science.org/data>

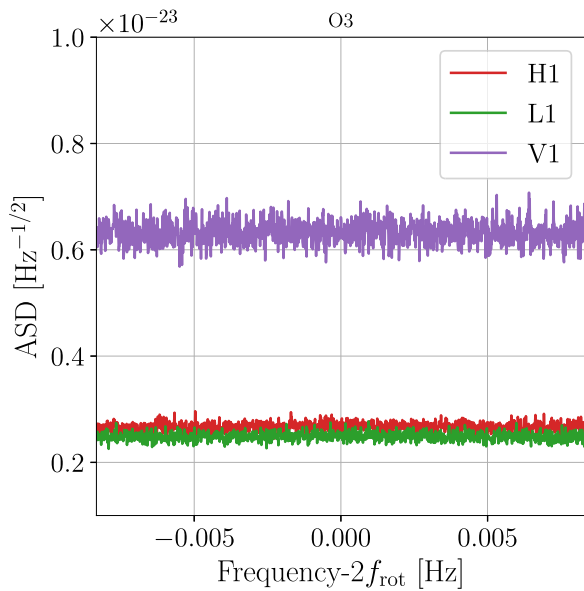


Figure 3. Two-sided amplitude spectral density (ASD) after heterodyning, low-pass filtering, and downsampling the raw strain data for the $l = m = 2$ gravitational-wave mode. Different color lines indicate the Hanford (H1), Livingston (L1), and Virgo (V1) detectors.

Q_{22} and d , we use flat priors that are bounded between zero and 1×10^{-22} , which is again well above the limit implied in Abbott et al. (2019a). To analyze multiple detectors’ data sets simultaneously, we combine the product of the Student’s t -likelihoods calculated for each detector (Dupuis & Woan 2005).

The outputs of the analysis are posterior distributions of the parameters of interest, which are $h_0/Q_{22}/\varepsilon$ for the single harmonic search, C_{21} and C_{22} for the dual harmonic search, and the angles $\cos \iota$ and ψ for both choices of priors. In Section 3, we present results on the amplitude parameters marginalized over the rest of the parameter space. We also provide odds ratios between two hypotheses: the data contain a coherent signal in the detectors, or incoherent signals or noise in the different detectors. These values are used to assess the presence of a signal in the data and, for a given prior choice, can be thought of as a “detection statistic.”

3. Results

Results from our searches do not show evidence for gravitational-wave emission from PSR J0537–6910 via the two models that we assume. For the single harmonic model, the Bayesian odds of the data containing a coherent signal between detectors versus incoherent signals or noise in the different detectors (see Equation (A6) of Abbott et al. 2017a) favor the latter case by $\sim 20,000$ and $\sim 31,000$ for the unrestricted and restricted priors, respectively. For the dual harmonic model, the case of an incoherent signal or noise in the detectors is favored by $\lesssim 2 \times 10^8$ for both prior choices.

An amplitude spectral density obtained after the heterodyne correction is displayed in Figure 3 for each of the three detectors. If a loud continuous gravitational-wave signal was present, we would expect to see a narrow line feature in the spectrum. The amplitude spectral densities also give an estimation of the sensitivity of the search.

Given the lack of evidence for a signal from either the single or dual harmonic models, we expect the odds between these

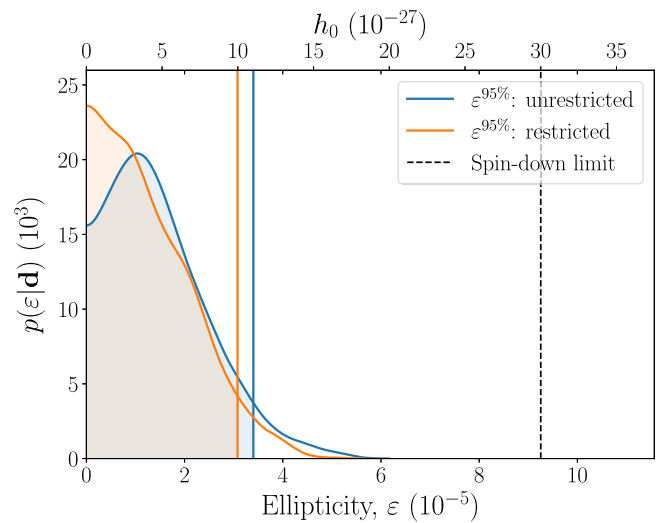


Figure 4. Posterior probability distribution for ellipticity and h_0 for the analyses with unrestricted and restricted priors on the pulsar orientation. The 95% credible upper limits are shown as vertical colored lines, while the spin-down limit is given by the vertical dashed black line.

Table 3

95% Upper Limits on Gravitational-wave Strain, Ellipticity, and Other Quantities Based on Unrestricted (UR) and Restricted (R) Choices for Priors on Polarization and Inclination Angles

Prior	$h_0^{95\%}$ (10^{-26})	$\varepsilon^{95\%}$ (10^{-5})	$h_0^{95\%}/h_0^{\text{sd}}$	$C_{21}^{95\%}$ (10^{-26})	$C_{22}^{95\%}$ (10^{-27})
UR	1.1	3.4	0.37	2.2	5.6
R	1.0	3.1	0.33	1.8	5.0

Note. Results here come from analyzing all O3 data and the last 6 days of O2 data.

models to favor the simpler single harmonic model. Indeed, we find that the single harmonic model is strongly favored by factors of ~ 5700 and ~ 9200 for the restricted and unrestricted orientation cases, respectively. However, it is worth noting that the odds between models will depend on our choice of the uniform prior range on the amplitude parameters.

Though no gravitational waves are detected, we can still determine upper limits on possible gravitational-wave emission from PSR J0537–6910. Here, we use 95% credible upper bounds on the amplitude parameters based on their marginalized probability distributions.²⁹³ The dimensionless gravitational-wave amplitude h_0 and coefficients C_{21} and C_{22} are constrained for the single and dual harmonic searches, respectively. For the single harmonic search, h_0 can be mapped to a limit on the maximum ellipticity ε using Equation (4). In Table 3, we show the different constraints for both searches using all O3 data and the last ~ 6 days of O2 data (see Section 2.3). In addition to the detector calibration uncertainties discussed in Section 2.3, we estimate that the statistical uncertainty on the upper limits due to the use of a finite number of posterior samples is on the order of 1%.

Figure 4 shows the marginalized posterior probability distributions on the pulsar ellipticity and h_0 for the single harmonic search

²⁹³ Simulations on independent and identically distributed noise realizations show that the different noise instantiations can produce upper limits that vary by $\sim 20\%$ at a 1σ confidence level. However, the Bayesian credible limits we present are valid for our particular data set.

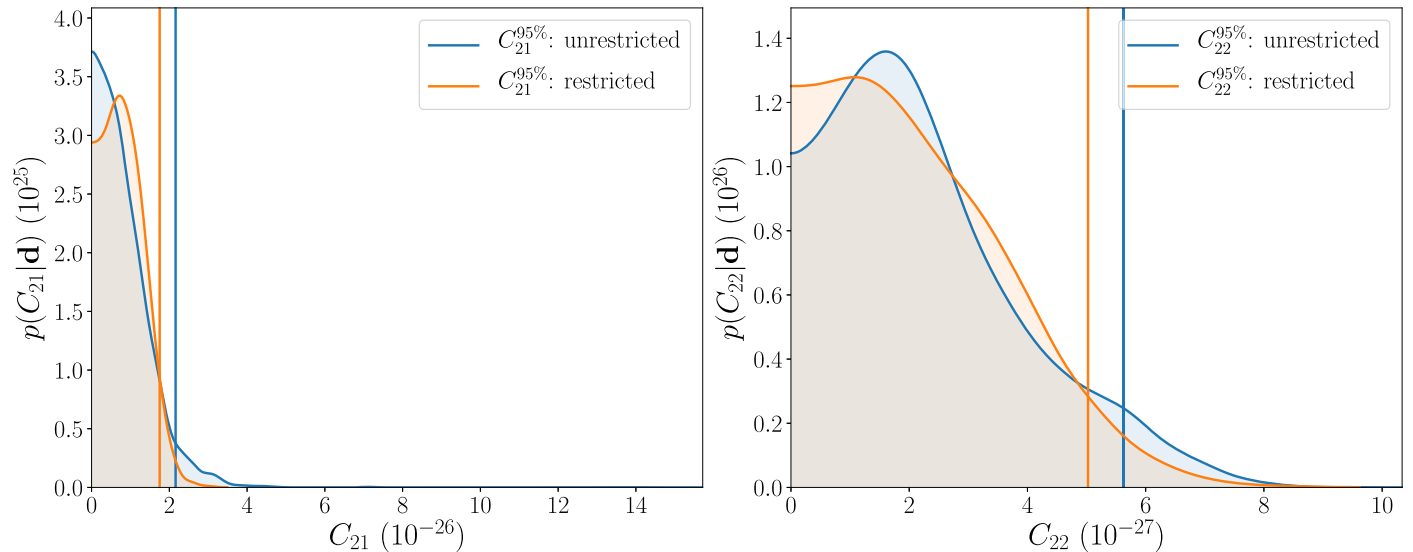


Figure 5. Posterior probability distributions for the amplitudes C_{21} and C_{22} with unrestricted and restricted priors on the pulsar orientation. The 95% credible upper limits are shown as vertical colored lines.

with unrestricted and restricted source orientation priors. The posteriors show significant support at ellipticities of zero, indicating no evidence of a signal at current sensitivities. We therefore show 95% credible upper limits on the ellipticity for both prior choices along with the fiducial spin-down limit.

Figure 5 shows a similar posterior distribution on the dimensionless amplitudes C_{21} and C_{22} for the dual harmonic model. For this model, no evidence of gravitational waves is found, so an upper limit at 95% is indicated in both panels of this figure. The model given by Equation (1) implies that the value of C_{21} becomes completely unconstrained when $\sin \iota = 0$. For the unrestricted orientation prior result shown in the left panel of Figure 5, this leads to a long high amplitude tail in the C_{21} posterior distribution. In Figures 4 and 5, we see that the amplitude posteriors can peak away from zero. This behavior was unsurprising and can occur even for pure Gaussian noise. Even with these peaks, the posteriors are still entirely consistent with zero ellipticity. For example, for the unrestricted posterior distribution shown in Figure 4, a value of zero ellipticity is within the minimum 66% credible interval around the mode.

In contrast to emission in the single harmonic case, an energy-based limit on gravitational-wave emission is rather complex in the dual harmonic case. The relevant constraint is that the observed spin-down energy is equal to the sum of the luminosities at the two harmonics. These two emissions have different beam patterns: the emission at the rotation frequency is strongest along the rotational equator ($\iota = \pi/2$ direction), where the polarization is linear, while emission at twice the rotation frequency is strongest along the axis of rotation ($\iota = 0$), where the polarization is circular. Therefore, the spin-down limit on the maximum amplitudes of the two harmonics depends on both the relative size of the intrinsic strength of the two components and the orientation of the spin axis relative to the observer. To provide some insight, if we compare the sky-averaged emission strength at only the rotation frequency to emission at only twice the rotation frequency, the spin-down limit would allow the amplitude of the radiation at the rotation frequency to be approximately twice as strong as that at twice the rotation frequency (see Section 3 of Jones 2010 for more details).

The results presented above use all O3 data in combination with about six days of O2 data, when NICER was operating and monitoring PSR J0537–6910. We also conducted searches using only O3 data or using O3 data plus O2 data from 2017 March 22 to the end of O2. The latter analysis assumes no glitches occurred during the additional time and represents the estimated maximum time that can be safely included without a contemporaneous timing model (see Section 2.3). For only O3 data, we obtain h_0 and ε limits that are worse by $\sim 7\%$ for the unrestricted prior and unchanged for the restricted prior, compared to those shown in Table 3. For O3 data plus the extra O2 data, we obtain amplitude limits that are improved by $\lesssim 20\%$ compared to those shown in Table 3.

4. Conclusions

Using data from LIGO/Virgo’s second and third observing runs, we searched for mass quadrupolar-sourced gravitational waves from the young, dynamic PSR J0537–6910 at once or twice the pulsar’s rotational frequency of 62 Hz. For the first time, we reached below the gravitational-wave spin-down limit for PSR J0537–6910 and showed that gravitational-wave emission for a pure $l=m=2$ mode accounts for less than 14% of the pulsar’s spin-down energy budget. We placed the third most stringent constraint on the ellipticity ($\varepsilon < 3 \times 10^{-5}$) of any young pulsar (behind only the Crab pulsar and B1951+32/J1952+3252; Abbott et al. 2019a, 2020). While this limit is much higher than those of old recycled millisecond pulsars (for which $\varepsilon < 10^{-8}$; Abbott et al. 2020), young pulsars such as PSR J0537–6910 and the Crab pulsar are important because they have much stronger magnetic fields (and are hotter) and thus might have greater ellipticities. The ellipticity constraint of PSR J0537–6910 is also above or near estimates of the maximum ellipticity that can be sustained by an elastically deformed neutron star crust (Johnson-McDaniel & Owen 2013; Caplan et al. 2018; Gittins et al. 2021).

PSR J0537–6910 is a frequently glitching pulsar and potential source of continuous gravitational waves. The X-ray data from NICER give us the necessary tools to account for the phase evolution of a gravitational-wave signal over time, which allows us to perform a fully coherent and sensitive search for

such a signal. While our multimessenger analysis focuses on gravitational waves from a time-varying mass quadrupole ($n = 5$), another search could be performed for gravitational waves from an r-mode fluid oscillation ($n = 7$) using wider-band techniques (e.g., Fesik & Papa 2020a, 2020b, using O2 data). The strain sensitivity achieved in our analysis (1×10^{-26}) is also comparable to the $(2 - 3) \times 10^{-26}$ estimated in Andersson et al. (2018) for r-mode emission from PSR J0537–6910.

Finally, from the observed correlation between glitch size and time to next glitch for PSR J0537–6910 (Middleditch et al. 2006; Antonopoulou et al. 2018; Ferdman et al. 2018; Ho et al. 2020b), we can hope to measure in the future low braking indices (7 or even lower) after the largest glitches. As noted above, braking indices of 5 and 7 are predicted by gravitational-wave-emitting mechanisms. The observed evolution of n_{ig} to lower values than those shown in Figure 1, which may occur after the effects of glitches on the pulsar’s spin-down behavior have decayed, may indicate that gravitational waves are continuously emitted between glitches. On the other hand, glitches may trigger detectable transient gravitational waves (Prix et al. 2011; Ho et al. 2020a; Yim & Jones 2020), and gravitational-wave searches at glitch epochs of other pulsars have been conducted (Keitel et al. 2019). It is therefore vital to continue to monitor the spin evolution of PSR J0537–6910, not only to obtain the timing ephemeris and measure braking indices, but also to know when this pulsar undergoes a glitch. Since the spin period of PSR J0537–6910 is only detectable at X-ray energies, NICER is the only effective means to perform the necessary observations. Fortunately NICER is anticipated to operate until at least late 2022, overlapping with the fourth observing run of LIGO/Virgo and KAGRA (Aso et al. 2013), which is likely to begin in 2022 and continue into 2023.

The authors gratefully acknowledge the support of the United States National Science Foundation (NSF) for the construction and operation of the LIGO Laboratory and Advanced LIGO as well as the Science and Technology Facilities Council (STFC) of the United Kingdom, the Max-Planck-Society (MPS), and the State of Niedersachsen/Germany for support of the construction of Advanced LIGO and construction and operation of the GEO600 detector. Additional support for Advanced LIGO was provided by the Australian Research Council. The authors gratefully acknowledge the Italian Istituto Nazionale di Fisica Nucleare (INFN), the French Centre National de la Recherche Scientifique (CNRS) and the Netherlands Organization for Scientific Research, for the construction and operation of the Virgo detector and the creation and support of the EGO consortium. The authors also gratefully acknowledge research support from these agencies as well as by the Council of Scientific and Industrial Research of India, the Department of Science and Technology, India, the Science & Engineering Research Board (SERB), India, the Ministry of Human Resource Development, India, the Spanish Agencia Estatal de Investigación, the Vicepresidència i Conselleria d’Innovació Recerca i Turisme and the Conselleria d’Educació i Universitat del Govern de les Illes Balears, the Conselleria d’Innovació Universitats, Ciència i Societat Digital de la Generalitat Valenciana and the CERCA Programme Generalitat de Catalunya, Spain, the National Science Centre of Poland, the Swiss National Science Foundation (SNSF), the Russian Foundation for Basic Research, the Russian Science Foundation, the European Commission, the European Regional

Development Funds (ERDF), the Royal Society, the Scottish Funding Council, the Scottish Universities Physics Alliance, the Hungarian Scientific Research Fund (OTKA), the French Lyon Institute of Origins (LIO), the Belgian Fonds de la Recherche Scientifique (FRS-FNRS), Actions de Recherche Concertées (ARC) and Fonds Wetenschappelijk Onderzoek - Vlaanderen (FWO), Belgium, the Paris Île-de-France Region, the National Research, Development and Innovation Office Hungary (NKFIH), the National Research Foundation of Korea, Industry Canada and the Province of Ontario through the Ministry of Economic Development and Innovation, the Natural Science and Engineering Research Council Canada, the Canadian Institute for Advanced Research, the Brazilian Ministry of Science, Technology, Innovations, and Communications, the International Center for Theoretical Physics South American Institute for Fundamental Research (ICTP-SAIFR), the Research Grants Council of Hong Kong, the National Natural Science Foundation of China (NSFC), the Leverhulme Trust, the Research Corporation, the Ministry of Science and Technology (MOST), Taiwan, and the Kavli Foundation. The authors gratefully acknowledge the support of the NSF, STFC, INFN, and CNRS for provision of computational resources.

This work was supported by MEXT, JSPS Leading-edge Research Infrastructure Program, JSPS Grant-in-Aid for Specially Promoted Research 26000005, JSPS Grant-in-Aid for Scientific Research on Innovative Areas 2905: JP17H06358, JP17H06361, and JP17H06364, JSPS Core-to-Core Program A. Advanced Research Networks, JSPS Grant-in-Aid for Scientific Research (S) 17H06133, the joint research program of the Institute for Cosmic Ray Research, University of Tokyo, National Research Foundation (NRF), and Computing Infrastructure Project of KISTI-GSDC in Korea, Academia Sinica (AS), AS Grid Center (ASGC) and the Ministry of Science and Technology (MoST) in Taiwan under grants including AS-CDA-105-M06, Advanced Technology Center (ATC) of NAOJ, and Mechanical Engineering Center of KEK.

We thank all essential workers who put their health at risk during the COVID-19 pandemic, without whom we would not have been able to complete this work.

D.An. acknowledges support from an EPSRC fellowship (EP/T017325/1). C.M.E. acknowledges support from FONDECYT/Regular 1171421 and USA1899-Vrdei 041931SSSA-PAP (Universidad de Santiago de Chile, USACH). W.C.G.H. acknowledges support through grants 80NSSC19K1444 and 80NSSC21K0091 from NASA. This work is supported by NASA through the NICER mission and the Astrophysics Explorers Program and uses data and software provided by the High Energy Astrophysics Science Archive Research Center (HEASARC), which is a service of the Astrophysics Science Division at NASA/GSFC and High Energy Astrophysics Division of the Smithsonian Astrophysical Observatory.

Facility: NICER.

References

- Aasi, J., Abadie, J., Abbott, B. P., et al. 2014, *ApJ*, **785**, 119
Aasi, J., Abbott, B. P., Abbott, R., et al. 2015, *CQGra*, **32**, 074001
Abbott, B. P., Abbott, R., Abbott, T. D., et al. 2017a, *ApJ*, **839**, 12
Abbott, B. P., Abbott, R., Abbott, T. D., et al. 2017b, *PhRvD*, **96**, 122004
Abbott, B. P., Abbott, R., Abbott, T. D., et al. 2019a, *ApJ*, **879**, 10
Abbott, B. P., Abbott, R., Abbott, T. D., et al. 2019b, *PhRvD*, **99**, 122002
Abbott, B. P., Abbott, R., Acernese, F., et al. 2010, *ApJ*, **713**, 671
Abbott, R., Abbott, T. D., Abraham, S., et al. 2020, *ApJL*, **902**, L21
Abbott, R., Abbott, T. D., Abraham, S., et al. 2021, *SoftX*, **13**, 100658

- Acernese, F., Agathos, M., Agatsuma, K., et al. 2015, *CQGra*, **32**, 024001
- Andersson, N., Antonopoulou, D., Espinoza, C. M., Haskell, B., & Ho, W. C. G. 2018, *ApJ*, **864**, 137
- Andersson, N., Jones, D. I., & Ho, W. C. G. 2014, *MNRAS*, **442**, 1786
- Antonopoulou, D., Espinoza, C. M., Kuiper, L., & Andersson, N. 2018, *MNRAS*, **473**, 1644
- Aso, Y., Michimura, Y., Somiya, K., et al. 2013, *PhRvD*, **88**, 043007
- Caplan, M. E., Schneider, A. S., & Horowitz, C. J. 2018, *PhRvL*, **121**, 132701
- Caride, S., Inta, R., Owen, B. J., & Rajbhandari, B. 2019, *PhRvD*, **100**, 064013
- Chen, Y., Wang, Q. D., Gotthelf, E. V., et al. 2006, *ApJ*, **651**, 237
- Dupuis, R. J., & Woan, G. 2005, *PhRvD*, **72**, 102002
- Ferdman, R. D., Archibald, R. F., Gourgouliatos, K. N., & Kaspi, V. M. 2018, *ApJ*, **852**, 123
- Fesik, L., & Papa, M. A. 2020a, *ApJ*, **895**, 11
- Fesik, L., & Papa, M. A. 2020b, *ApJ*, **897**, 185
- Gao, Y., Shao, L., Xu, R., et al. 2020, *MNRAS*, **498**, 1826
- Gendreau, K. C., Arzoumanian, Z., & Okajima, T. 2012, *Proc. SPIE*, **8443**, 844313
- Gittins, F., Andersson, N., & Jones, D. I. 2021, *MNRAS*, **500**, 5570
- Glampedakis, K., & Gualtieri, L. 2018, in *Gravitational Waves from Single Neutron Stars: An Advanced Detector Era Survey*, Astrophysics and Space Science Library, Vol. 457, ed. L. Rezzolla et al. (Dordrecht: Springer), **673**
- Ho, W. C. G., Espinoza, C. M., Arzoumanian, Z., et al. 2020b, *MNRAS*, **498**, 4605
- Ho, W. C. G., Jones, D. I., Andersson, N., & Espinoza, C. M. 2020a, *PhRvD*, **101**, 103009
- Idrisy, A., Owen, B. J., & Jones, D. I. 2015, *PhRvD*, **91**, 024001
- Jaranowski, P., Królak, A., & Schutz, B. F. 1998, *PhRvD*, **58**, 063001
- Johnson-McDaniel, N. K., & Owen, B. J. 2013, *PhRvD*, **88**, 044004
- Jones, D. I. 2010, *MNRAS*, **402**, 2503
- Jones, D. I. 2015, *MNRAS*, **453**, 53
- Keitel, D., Woan, G., Pitkin, M., et al. 2019, *PhRvD*, **100**, 064058
- Manchester, R. N., Hobbs, G. B., Teoh, A., & Hobbs, M. 2005, *AJ*, **129**, 1993
- Marshall, F. E., Gotthelf, E. V., Middleditch, J., Wang, Q. D., & Zhang, W. 2004, *ApJ*, **603**, 682
- Marshall, F. E., Gotthelf, E. V., Zhang, W., Middleditch, J., & Wang, Q. D. 1998, *ApJL*, **499**, L179
- Middleditch, J., Marshall, F. E., Wang, Q. D., Gotthelf, E. V., & Zhang, W. 2006, *ApJ*, **652**, 1531
- Mytidis, A., Coughlin, M., & Whiting, B. 2015, *ApJ*, **810**, 27
- Mytidis, A., Panagopoulos, A. A., Panagopoulos, O. P., Miller, A., & Whiting, B. 2019, *PhRvD*, **99**, 024024
- Ng, C.-Y., & Romani, R. W. 2008, *ApJ*, **673**, 411
- Owen, B. J. 2005, *PhRvL*, **95**, 211101
- Pietrzyński, G., Graczyk, D., Giallenne, A., et al. 2019, *Natur*, **567**, 200
- Pitkin, M., Gill, C., Jones, D. I., Woan, G., & Davies, G. S. 2015, *MNRAS*, **453**, 4399
- Prix, R., Giampanis, S., & Messenger, C. 2011, *PhRvD*, **84**, 023007
- Riles, K. 2017, *MPLA*, **32**, 1730035
- Shapiro, S. L., & Teukolsky, S. A. 1983, *Black Holes, White Dwarfs, and Neutron Stars: the Physics of Compact Objects* (New York: Wiley-Interscience)
- Sun, L., Goetz, E., Kissel, J. S., et al. 2020, *CQGra*, **37**, 225008
- Vallisneri, M., Kanner, J., Williams, R., Weinstein, A., & Stephens, B. 2015, *JPhCS*, **610**, 012021
- Veitch, J., Raymond, V., Farr, B., et al. 2015, *PhRvD*, **91**, 042003
- Veitch, J., & Vecchio, A. 2010, *PhRvD*, **81**, 062003
- Wang, Q. D., & Gotthelf, E. V. 1998, *ApJ*, **494**, 623
- Yim, G., & Jones, D. I. 2020, *MNRAS*, **498**, 3138